



Universität für Bodenkultur Wien

# *IN VITRO* EXPRESSION OF THE MEMBRANE PROTEIN LamB INTO POLYMERIC MEMBRANE ARCHITECTURES

Masterarbeit

an der Universität für Bodenkultur Wien

Department für Nanobiotechnologie

Institut für Synthetische Bioarchitekturen

Vorstand: Univ.Prof. Dr.rer.nat. Eva-Kathrin Sinner

Betreuerin: Univ.Prof. Dr.rer.nat. Eva-Kathrin Sinner

Co-Betreuer: Dipl.Chem. Dr. Christoph Zaba

Eingereicht von  
Fabio Bisaccia, BSc.

Wien, Februar 2017

## **Acknowledgement**

I want to thank my parents **Rocco** and **Marianne Bisaccia** for their support, as well as **Eva-Kathrin Sinner** and **Christoph Zaba** for their supervision.

# 1 Table of content

1 Table of content .....	2
2 Introduction .....	4
2.1 Motivation .....	4
2.2 Current limitations .....	4
2.2.1 Membrane protein purification .....	4
2.2.2 The need for a lipid membrane substitute .....	5
2.3 Strategies applied in this thesis .....	5
2.4 State of the art .....	7
2.5 Membrane proteins .....	7
2.6 Maltoporin .....	8
3 Results .....	9
3.1 Designing and characterization of pBSK(+) .....	9
3.1.1 Design of pBSK(+) .....	9
3.1.2 Characterization of pBSK(+) .....	9
3.2 pBSK(+) amplification and purification .....	10
3.2.1 Transformation of E. coli and plate culture .....	10
3.2.2 Liquid culture .....	11
3.2.3 Small scale plasmid purification .....	11
3.3 Attempts to increase plasmid yield .....	11
3.3.1 Medium scale plasmid purification .....	12
3.3.2 Medium scale plasmid purification with new kit .....	12
3.3.3 Optimized plasmid purification protocol .....	16
3.4 Testing the S30 T7 HighYield kit using VDAC .....	17
3.5 IVS without purification .....	17
3.6 IVS and post-synthesis purification methods .....	18
3.6.1 Antibody-modified silica nano-particles .....	18
3.6.2 Dialysis with 25 kDa and 50 kDa cut-offs .....	20
3.6.3 Dialysis with 100 kDa cut-off .....	21
3.7 IVS with optimized purification method .....	23
3.8 Separation LamB and LMP through low voltage SDS-PAGE .....	24
3.9 Separation of LamB and LMP through fluorescent amino acids .....	25
3.10 Mass spectrometry .....	26
3.11 DNA sequencing analysis of pBSK(+) .....	27
4 Material and Methods .....	29
4.1 Designing and ordering pBSK(+) .....	29
4.2 DNase digest of pBSK(+) .....	30
4.3 Primer design for PCR .....	30
4.4 PCR .....	30

4.5 Transformation of <i>E. coli</i> .....	31
4.6 Liquid culture .....	31
4.7 Plasmid purification .....	32
4.8 Absorption measurement .....	32
4.9 Vacuum assisted concentration .....	32
4.10 Refined liquid culture and plasmid purification .....	32
4.11 Testing the IVS kit .....	32
4.12 SDS-Page .....	33
4.13 Protein staining.....	33
4.14 DNA gel and electrophoresis set-up .....	33
4.15 IVS without purification .....	34
4.16 Antibodies (Abs) .....	34
4.17 Immuno-functionalised silica nanoparticles.....	34
4.18 Purification with SiNPs (anti PEG) .....	36
4.19 25 kDa and 50 kDa membranes .....	37
4.20 100 kDa membrane .....	37
4.21 Dialysis with 25 kDa and 50 kDa membranes.....	37
4.22 Polymersome synthesis.....	38
4.22.1 Polymersome synthesis through solvent exchange.....	38
4.22.2 Polymersome synthesis through polymer film rehydration.....	38
4.22.3 Polymersome synthesis through Electroformation.....	39
4.23 Sample preparation for transmission electron microscopy .....	39
4.24 Transmission electron microscopy.....	39
4.25 IVS with optimized purification method .....	40
4.26 Confocal laser microscopy.....	40
4.27 SDS-PAGE at reduced voltage.....	40
4.28 Fluorescent amino acids.....	41
4.29 Mass spectroscopy.....	41
4.30 Analysis of pBSK(+) sequencing data.....	41
5 Discussion .....	43
5.1 Optimisations .....	43
5.2 Reflections about possible improvements of future experiment design .....	43
5.2.1 Demand of sceptical handling of material.....	44
5.2.2 The importance of efficient detection methods .....	44
6 Supplemental information .....	46
6.1 Results from protein sequencing via mass spectrometry .....	46
7 Bibliography .....	49

## 2 Introduction

### 2.1 Motivation

One third of all human genes encodes for membrane proteins and more than 50 % of all pharmacologically active substances interact with membrane proteins.<sup>1</sup> But it is not only these remarkable numbers and their importance in medical application that explains the current focus in scientific research on membrane proteins. Proteins of this class are involved in numerous cellular functions and oftentimes provide means of communication and transportation between a cell and its surroundings.<sup>2, 3, 4, 5</sup>

Communication may thereby occur within an organism, as it is the case with receptor proteins, e.g. insulin receptors on liver cells, where a signal is transduced from the blood into the cell through a membrane protein.<sup>2</sup> To give an example of inter-species communication, some bacteria such as *Pseudomonas aeruginosa*<sup>6</sup> communicate via the release of so-called autoinducers.<sup>3</sup> These signalling molecules are recognized through receptor membrane proteins on other bacteria and trigger changes in gene-expression.

A second task fulfilled by membrane proteins is transportation across the cell membrane. The cargo may be information as well as a chemical substance, both of which are unable to pass the membrane without the help of said protein class. An example for transport of information is provided by membrane proteins such as the taste receptors found on mammalian tongues.<sup>4</sup> Taste receptors detect several different sapid molecules and forward the information about their presence to the cell. The bacterial outer membrane protein LamB serves as example for molecular transport across the membrane.<sup>5</sup> This channel protein forms a pore through the lipid bilayer, allowing only certain sugars to pass through.<sup>7</sup>

The selectivity regarding their cargo renders channel proteins such as LamB a useful tool in nanoscience, where they allow controlled transport of mass.<sup>8</sup> Pore proteins already find use in novel DNA sequencing methods and are a promising tool in loading of nano-containers for gene-therapy, to name two examples.<sup>9,5</sup>

As pointed out above, membrane proteins present not only great importance in medical terms, but are also involved in a multitude of cellular processes and show potential in nanoscience. However, *in situ* studies are oftentimes unfeasible due to a biological membrane's complexity.<sup>10</sup> This explains an increasing demand for functional and purified membrane proteins for research in these respective fields.

### 2.2 Current limitations

#### 2.2.1 Membrane protein purification

According to Lin and Guidotti, two obstacles have to be overcome in order to achieve enrichment of functional membrane proteins from cellular starting material: comparable low levels found in cells, and complications related to the use of detergents in order to isolate and purify membrane proteins from the original membrane context.<sup>11</sup>

Most membrane protein species are present in lower numbers per cell than soluble proteins.<sup>12</sup> Raising the natural levels through overexpression is oftentimes impossible, as cytotoxic effects are triggered by doing so.<sup>12</sup> This requires for large cell culture volumes as starting material, making the experiment more expensive and increasing the amount of work.

After a sufficient amount of cells is acquired and homogenised, another challenge has to be faced: the membrane protein of interest has to be solubilised. Only in solubilised form, i.e. freed from remaining membrane lipids, the protein can undergo further purification.<sup>10</sup> Solubilisation is usually achieved through the addition of amphiphilic detergents. As a result,

dissolved “lipid/protein/detergent complexes”<sup>11</sup> are formed. These complexes are depleted of lipids by further addition of detergent until only detergent stabilised membrane proteins remain in solution. This coat of detergents, however, gives rise to certain complications in the following procedure. Activity assays for transport proteins, for instance, may be affected by the presence of detergents.<sup>11</sup> Some detergents, such as Triton X-100 or Tween cause wrong results in the Bradford assay.<sup>11</sup> Furthermore purification methods such as reverse phase chromatography or ion exchange chromatography may not be suitable for protein/detergent complexes. The former due to the hydrophobicity of most detergents, the latter due to the obscuring effect of a detergent micelle on the net charge of a membrane protein surface.<sup>11</sup> The detergent molecules associated with the membrane protein also increase the apparent molecular weight when using gel chromatography.<sup>11</sup> It should further be mentioned, that a suitable detergent for each membrane protein species has to be empirically determined. This time-consuming task in addition with the limitations mentioned before, renders the use of detergents for membrane protein solubilisation a costly, time intensive and in some cases impossible purification method.<sup>11</sup>

### 2.2.2 The need for a lipid membrane substitute

After the initial hurdle of membrane protein purification is overcome, a second issue has to be faced. In order to maintain a membrane protein's native function, its structure has to be conserved. Since the structure depends on the protein's environment, a suitable support has to be provided to mimic a biological lipid membrane. Liposomes, spherical vesicles formed by a lipid double layer, are generally used as said support as they help to mimic the membranous context and, thus, prevent aggregation.<sup>10</sup> Although representing a useful tool due to their ability to self-assemble in aqueous solution, liposomes come with a drawback. According to Bermudez et al.<sup>13</sup>, the small thickness of the liposomes lipid layer of 3 to 5 nm renders them fragile, thus “practical applications involving liposomes have been continually hindered by a lack of stability”.<sup>13</sup> Lee and Feijen<sup>14</sup> furthermore report that liposomes are unstable during circulation in the mammalian body, limiting their capability as drug delivery devices in medical applications.

## 2.3 Strategies applied in this thesis

To circumvent the issues mentioned earlier surrounding membrane protein purification, two different techniques were applied in this thesis. Namely, *in vitro* synthesis (IVS) of proteins and the use of polymersomes as membrane mimicking architectures for synthesis of functionally folded membrane proteins. In the following, both techniques are elucidated and compared to cell-based protein expression and the use of liposomes.

For *in vitro* synthesis of proteins, cell lysates are used instead of living cells.<sup>12</sup> These lysates contain the necessary transcription and translation machinery, but are depleted of endogenous DNA and mRNA. Additionally, energy components to drive the protein production, as well as free amino acids are supplemented. IVS systems capable of performing transcription and (in subsequence) translation are called coupled systems. Systems on the other side that only carry out translation and depend on an external source of mRNA are known as linked systems.<sup>12</sup> *In vitro* synthesis is therefore initiated differently for coupled and linked reactions, by adding either DNA or mRNA template to the mixture.<sup>15</sup> The schematic principle of cell-free protein production is depicted in Figure 1.

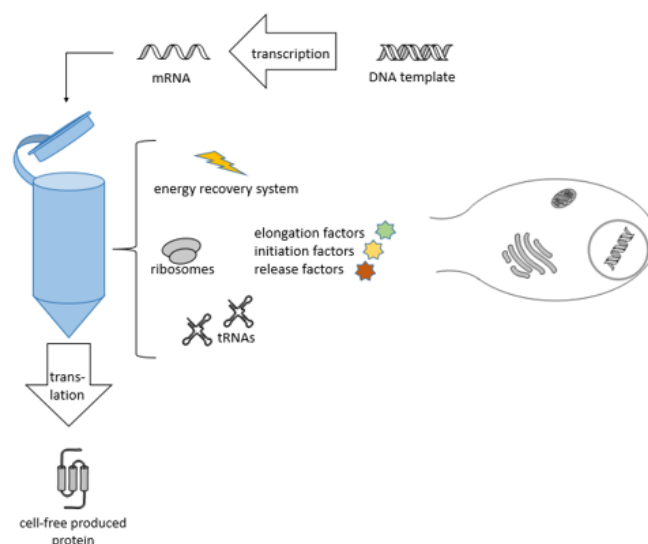


Figure 1 General pathway of cell-free *in vitro* protein synthesis.

The general principle shown above applies to all commercially available IVS kits, even though they are derived from different cell types.<sup>12</sup> According to Zemella et al.<sup>15</sup>, prokaryotic as well as eukaryotic cells are processed into *in vitro* synthesis reaction systems. Among the former, *Escherichia coli* derived lysates are one of the first developed systems. After over 60 years of improvements regarding removal of inhibitory by-products, energy regeneration and purity of components, however, the lack of post-translational modifications sets a clear limit to the use of these systems<sup>15</sup>. Eukaryotic cell-free systems, by contrast, are better suited in that regard. Wheat germ, insect and Chinese hamster ovary cell extracts for instance are capable of post-translational modification of synthetically (i.e. *in vitro*) produced proteins.<sup>15</sup>

After elucidating the principle of IVS extract-based protein production, the advantages of these techniques over cell-based synthesis of membrane proteins shall be discussed. Firstly, IVS does not depend on large amounts of crude cell mass from which the protein of interest is extracted. Unlike cell-based approaches, high expression does not harm the system, even when cytotoxic proteins are expressed.<sup>12</sup> Secondly, no detergents have to be used to break down a cell membrane or to solubilize the protein.<sup>16,17</sup> Furthermore, several other advantages of IVS of membrane proteins can be listed. The absence of cells allows for example to efficiently funnel resources into protein production, instead of cell growth.<sup>18</sup> Low reaction volumes in the range of microliters and high production efficiency with yield of milligrams per millilitre are possible.<sup>17</sup> This small scale makes it possible for the operator to control the levels of low-molecular weight compounds, facilitating labelling experiments (e.g. supplementing labelled aminoacyl-tRNA).<sup>17</sup> However, upscaling may be carried out to volumes up to 100 L.<sup>15</sup> Lastly, the simplified template preparation can be mentioned as an advantage. Plasmid DNA, PCR products and mRNA as possible feeds allow for a flexible experimental design. Furthermore, selection markers, template replication and template stability are of less concern in *in vitro* synthesis of proteins.<sup>17</sup>

As mentioned earlier, polymersomes were chosen as membrane equivalent supports for membrane proteins in this work. These artificial structures are vesicles made of amphiphilic block copolymers. Block copolymers consist of several homopolymer blocks that are covalently linked.<sup>14</sup> These polymers possess the ability to self-assemble into different complex structures including polymersomes<sup>13</sup>, which provide several advantages over liposomes in applications involving membrane proteins. Firstly, their enhanced robustness due to a thicker membrane<sup>13</sup> causes long-time stability in the order of years.<sup>5</sup> Secondly, a higher stability was also observed *in vivo*, as was reported by Lee et al.<sup>14</sup> This includes a longer blood circulation time, a necessary trait for a potential drug delivery vehicle.<sup>14</sup> Therefore, polymersomes provide a stable support for membrane proteins by mimicking biological membranes.<sup>5</sup>

## 2.4 State of the art

Graff et al.<sup>5</sup> purified the *Shigella sonnei* variant of membrane protein LamB from the expression host *Escherichia coli* by detergent solubilisation. The protein was then incorporated into small unilamellar triblock copolymer vesicles. LamB was thereby chosen for its unique interactions with the  $\lambda$  phage. The phage naturally recognises and binds LamB. It subsequently injects its DNA cargo across the membrane into the cell using the protein. Graff et al. successfully showed that LamB embedded in a polymeric membrane still possessed the ability to be bound by the phage. Furthermore, injection of the viral DNA through the membrane into the polymersome was observed. It was therefore concluded, that LamB maintained its natural conformation even when being inserted into a polymeric membrane. The group presented their findings as promising tool for efficient loading of “nanocontainers” that could be used in gene therapy applications.<sup>5</sup>

The goal of this thesis was to replicate the incorporation of functional LamB into polymersomes, however, through *in vitro* synthesis instead of traditional cell-based expression of the membrane protein. This would allow to combine the possibility to load nanocontainers via phages with the benefits of IVS technology that were outlined in the previous section.

## 2.5 Membrane proteins

As membrane proteins represent a central theme in this work, the interested reader will find a rundown to this protein class in the following to deepen his or her understanding of the topic.

As stated by Tan et al.<sup>19</sup>, biological membranes represent a barrier between cells and their respective environment. In the case of eukaryotes, biological membranes further define organelles, compartments of specialised function, inside the cell. As borders between heterogeneous environments, these membranes are architectures with crucial and unique functions. Among said functions, signal transduction, anchorage of the cytoskeleton, energy production and molecular transport can be listed. The agents carrying out these tasks are proteins associated to the membrane, known as membrane proteins. As the functional part of a biological membrane, these proteins in average make up about 50 % of the membrane mass.<sup>19</sup> It is further estimated that one third of all naturally occurring proteins belongs to the family of membrane proteins. This plethora of membrane proteins is generally subdivided into two branches: peripheral and integral membrane proteins. Both types are schematically depicted in Figure 2.

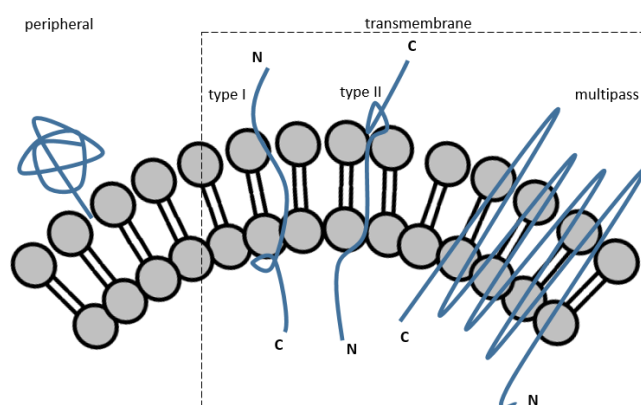


Figure 2 Membrane proteins are classified into peripheral membrane proteins and transmembrane proteins (dashed box). Transmembrane protein are subdivided into type I, type II and multipass proteins.

Integral membrane proteins, also referred to as transmembrane proteins, are of particular interest in this work. They are further sub-classified into type I, type II and multipass proteins



(Figure 2). All three types pierce through the lipid bilayer at least with one single transmembranal domain. The membrane spanning regions of type I and II are hereby composed of hydrophobic amino acids that form an  $\alpha$ -helix. In the case of a type I transmembrane protein, the N-terminus is facing the exterior, whereas the C-terminus looms into the interior. Type II proteins present the opposite case with the C-terminus on the outside. The third type, multipass proteins, possesses several membrane spanning regions per protein. Some multipass proteins form  $\beta$ -barrel structures, thereby creating aqueous pores through the hydrophobic membrane. Such structures often serve as molecular transporters across the membrane.<sup>19</sup>

## 2.6 Maltoporin

The membrane protein LamB of *Shigella sonnei* and its *in vitro* synthesis are the central theme of this thesis. LamB, also known as maltoporin<sup>7</sup>, is naturally found in Gram-negative bacteria's outer-membrane.<sup>20</sup> There, the 446 amino acid<sup>21</sup> long protein forms a  $\beta$ -barrel of 18 antiparallel strands<sup>7</sup>, embedded into the lipid membrane. This barrel-like shape encompasses a pore of 5 Å diameter which stretches through the lipid bilayer.<sup>7</sup> The  $\beta$ -barrel's strands are connected by long loops on the cell's outside, and shorter ones on the interior of the cell.<sup>7</sup> Maltoporin naturally forms a homotrimeric structure as seen in Figure 3.

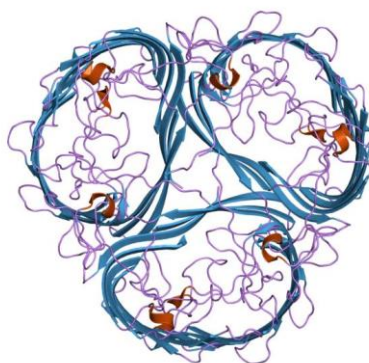


Figure 3 Top-down view on a maltoporin trimer (i.e. from the cell's exterior towards its interior), comprised of three molecules, each forming a  $\beta$ -barrel.<sup>22</sup> (image taken from <http://www.ebi.ac.uk/>)

As the two names, i.e. maltoporin and LamB, suggest, two major functions are carried out by this membrane protein.

The name maltoporin, was given to the protein in 1975<sup>7</sup> due to its function as substrate-specific channel for maltose and maltodextrin.<sup>20</sup> Diffusion of said ligands leads through the central pore of each monomer.<sup>7</sup> The pore comprises the so-called “greasy slide”, a helical stretch of aromatic amino acids, as well as the “polar tracks”, polar amino acid residues.<sup>7</sup> Both the slide and the tracks provide a continuous path of binding partners for the transported molecule.<sup>7</sup>

The second name in literature, LamB, was given to the protein upon its discovery in 1973 as the  $\lambda$ -phage receptor.<sup>7</sup> This bacteriophage injects its DNA into the host cell<sup>5</sup>, after binding to the exposed loops of the protein on the cell surface.<sup>7</sup> How exactly the viral DNA passes through the membrane is unknown. What is known is that the pore formed by the  $\beta$ -barrel is too narrow to serve as DNA channel.<sup>8</sup>

## 3 Results

### 3.1 Designing and characterization of pBSK(+)

#### 3.1.1 Design of pBSK(+)

A suitable expression vector for *in vitro* synthesis (IVS) of LamB should provide the following four features. An origin of replication (ORI) is required to amplify the plasmid after transformation into *E. coli*. The vector should carry an antibiotic resistance to select for successful transformations. Furthermore, the T7 promotor should be positioned upstream of the multiple cloning site (MCS). Lastly, the cDNA of LamB from *Shigella sonnei* should be cloned into the MCS under the control of the T7 promotor.

The bluescript SK+ (pBSK(+)) plasmid fulfilled the first three requirements and was therefore chosen as expression vector. Cloning of maltoporin's cDNA sequence into the MCS was already carried out by the manufacturer.

#### 3.1.2 Characterization of pBSK(+)

Before usage in *in vitro* synthesis, the delivered plasmid pBSK(+) was characterized via DNase digest and polymerase chain reaction (PCR).

##### 3.1.2.1 DNase digest

The whole plasmid had a size of 3985 base pairs (bp) and carried two cutting sites recognized by restriction enzyme HindIII at position 2211 and 3311. Digestion should therefore yield two equimolar fragments: a larger 2885 bp long stretch, and a smaller 1100 bp long one.

After DNase treatment the sample was transferred onto an agarose gel where they underwent electrophoresis. DNA bands were subsequently visualized under UV-light. As seen in Figure 4, the result was in good accordance with the expected outcome.

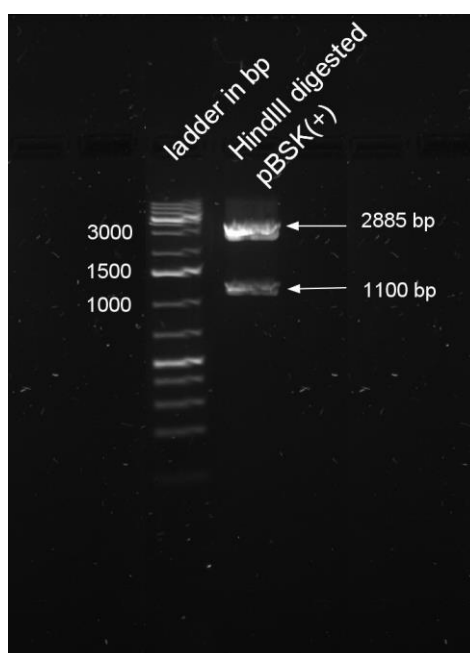


Figure 4 After digestion with HindIII two fragments appeared on the electrophoresis gel (white arrows).

### 3.1.2.2 PCR

Successful insertion of the LamB cDNA was investigated by PCR. Two primers, forward and backwards, were designed to target maltoporin's open reading frame (ORF). The forward primer bound at the 5' end of the coding strand, whereas the reverse primer associated with the 5' end of the non-coding strand. Figure 5 depicts the primers binding location schematically.

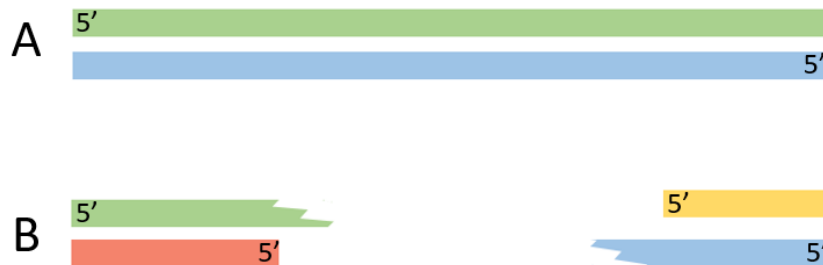


Figure 5 A: Coding strand (green) and non-coding strand (blue) of LamB. B: The forward primer (red) binds the coding strand at its 5' end. The reverse primer (yellow) binds the non-coding strand at its 5' end.

Primers and template were added to a PCR reaction sample. The reaction mix was subsequently analysed by DNA gel electrophoresis. A 1190 bp long DNA product was expected. The resulting gel is depicted in Figure 6. The obtained band appeared with the expected length.

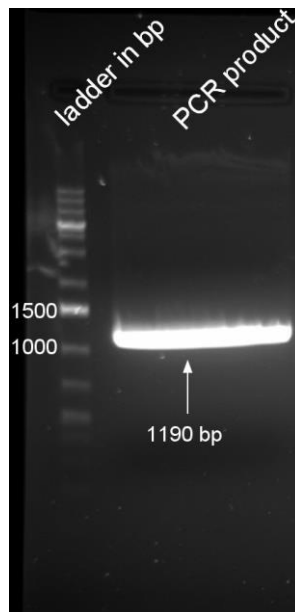


Figure 6 PCR produced a DNA fragment of the expected length.

## 3.2 pBSK(+) amplification and purification

### 3.2.1 Transformation of *E. coli* and plate culture

The competent *E. Coli* strain OneShot TOP10 was transformed with pBSK(+) via heat shock treatment. Upon transformation the bacterial cells were transferred unto three agar plates containing the antibiotic ampicillin. The plates were cultivated overnight at 37° C.

### 3.2.2 Liquid culture

On two of three plates colony formation was observed. From each successful plate one colony was picked and transferred into one respective liquid culture of 4 mL LB Medium plus ampicillin. The cultures were cultivated in a shaker with 180 rpm and 37° C overnight. The medium turned turbid, indicating successful growth.

### 3.2.3 Small scale plasmid purification

The overnight cultures were processed via a small scale plasmid purification kit to extract the plasmid. Liquid cultures were treated according to manufacturer's manual. This procedure yielded two times 50  $\mu$ L of plasmid solution, whose DNA content was subsequently measured via absorption spectroscopy using a NanoDrop device. For this purpose, 1.5  $\mu$ L aliquots were taken from each sample. Measurements were repeated three times. Resulting mean values from these measurements are listed in Table 1.

Table 1 Results from NanoDrop measurement after small scale plasmid purification.

Sample	260 / 280	260 / 230	DNA concentration [ng / $\mu$ L]	total DNA mass [ $\mu$ g]
A	1.95	2.01	74.1	3.71
B	1.89	2.05	75.5	3.78

The average DNA concentration of both samples was 74.8 ng/ $\mu$ L. This value was too low, since following *in vitro* synthesis batches were limited to a total volume of 50  $\mu$ L and therefore required a plasmid concentration of several hundred nanogram per microliter. The total DNA mass of both samples combined was 6.81  $\mu$ g. To guarantee time efficient experimenting, a total mass of at least 20 micrograms was desired, as one IVS reaction alone demands about 1  $\mu$ g plasmid material.

Plasmid concentration as well as total plasmid mass were therefore not sufficiently high to perform *in vitro* synthesis at this point in time and the attempt was made to obtain higher yields.

### 3.3 Attempts to increase plasmid yield

After the small scale plasmid purification proved non-viable, different approaches were undertaken to increase the plasmid yield from liquid culture in terms of DNA mass and DNA concentration: vacuum-assisted concentration, uniting plasmid purification product volumes, increasing initial cell mass and up-scaling to a medium sized plasmid purification kit.

In order to increase DNA concentration small scale purification derived plasmid solutions were placed in a vacuum concentrator. Over the course of one hour, the following increase in concentration was observed by absorption spectroscopy measurements and is listed in Table 2.

Table 2 Results of absorption spectroscopy measurements before and after vacuum evaporation.

Sample	260 / 280	260 / 230	Volume [ $\mu$ L]	DNA concentration [ng / $\mu$ L]
C	1.84	0.96	50	40.0
C after 1 h	1.78	1.07	20	96.2

Although this approach proved to be a useful tool to increase the plasmid concentration significantly over a short time, the achieved final concentration of 96.2 ng/ $\mu$ L was still too low. Furthermore, the associated rise in salt concentration rendered this method disadvantageous.

The maximal volume of cell culture to be processed by small scale plasmid purification is limited to 2 mL by the dimensioning of the kit. To increase the amount of input cell solution, four parallel purification batches of 2 mL were treated. The products of all four purifications were united and measured via absorption spectroscopy. These results are given in Table 3.

*Table 3 Absorption spectroscopy measurement results of four small scale plasmid purification batches united into one volume.*

Sample	260 / 280	260 / 230	DNA concentration [ng / $\mu$ L]	total DNA mass [ $\mu$ g]
D	1.79	1.77	44.3	2.22

Since running several small scale purification batches in parallel and uniting the products did not lead to an increase in total harvested mass of plasmids, a new concept was tried out.

Eight times 2 mL overnight culture were pelleted through centrifugation. Four pellets each were united and re-suspended to increase cell feed mass. The small scale plasmid purification protocol was then followed through as if just 2 mL of bacterial culture were being processed. Plasmid concentrations were evaluated subsequently using absorption spectroscopy. Resulting values are listed in Table 4.

*Table 4 DNA concentration measurement after uniting four cell pellets and performing small scale plasmid purification.*

Sample	260 / 280	260 / 230	DNA concentration [ng / $\mu$ L]	total DNA mass [ $\mu$ g]
E	1.96	1.07	24.1	1.2
F	1.84	0.96	40.0	2

The amount and concentration of purified plasmid was still below the desired values. Since all of the methods mentioned above were based on small scale purification kits, medium scale kits were utilized in the following instead for their ability to process larger volumes.

### 3.3.1 Medium scale plasmid purification

Overnight cultures were produced as described in chapter 3.2.2, but with a larger volume of 25 mL of medium. Plasmid purification was performed as instructed in the manufacturer's manual.

Subsequent photometric DNA concentration measurements, however, did not detect any absorption at 260 nm. The experiment was rerun four times, yielding no detectable plasmids.

### 3.3.2 Medium scale plasmid purification with new kit

To exclude a possible dysfunction of the used kit, a new one was bought from the same provider. However, there was still no detectable plasmid after processing an overnight culture through the new kit.

Since all the liquid cultures used were seeded from the same plate culture and incubated under identical conditions, it was assumed that plasmids were indeed present, but got lost during the purification process. To define the exact step, in which the loss occurred, samples were taken

after each step of the medium scale plasmid purification protocol.<sup>23</sup> Said protocol is listed in Table 5 to facilitate understanding of the origins of samples.

Table 5 Protocol for medium scale plasmid purification from liquid culture.

1	Harvesting cells from overnight culture by centrifugation.
2	Resuspension of bacterial pellet in 4 mL buffer.
3	Adding 4 mL lysis buffer, mixing, incubation at room temperature.
4	Adding 4 mL neutralization buffer, mixing, incubation on ice.
5	Centrifugation of cell debris.
6	Equilibrating column.
7	Applying supernatant from 5 to column.
8	Washing the column with 20 mL washing buffer (QC).
9	Eluting DNA with 5 mL elution buffer (QF).
10	Precipitating DNA by adding 3.5 mL isopropanol. Centrifugation.
11	Washing the pellet with 70 % ethanol.
12	Drying pellet. Redissolving DNA in 50 $\mu$ L TAE buffer.

Possible plasmid losses could appear in step 7, 8, 9 or 10. The balance of influx and flow through of these critical steps is schematically depicted in Figure 7.

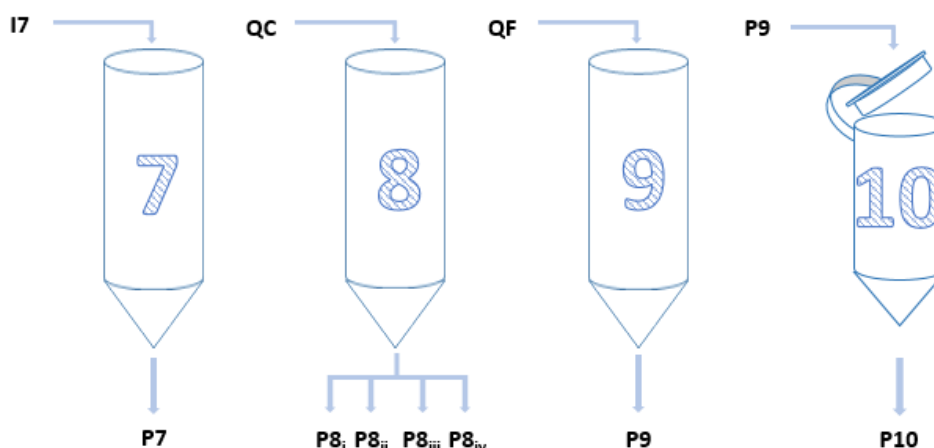


Figure 7 Influxes and outputs of the purification steps 7 to 10.

The influx of step seven 7 (I7) consists of the supernatant of step 5. The resulting permeate was labelled P7. QC buffer serves as input flow in step 8, and was named P8<sub>i</sub> to P8<sub>iv</sub> once it had passed through the column. P8<sub>i</sub> contains the first 5 mL of flow-through, P8<sub>ii</sub> the second 5 mL and so on. QF buffer was applied in step 9. The permeate of this step was labelled P9. P9 underwent precipitation of DNA and centrifugation to yield P10.

Samples I7, P7, P8<sub>i</sub> – P8<sub>iv</sub>, P9 and P10 were measured via absorption photometry. The results are listed in Table 6 DNA concentration measurement of the plasmid purification's intermediate samples.

Table 6 DNA concentration measurement of the plasmid purification's intermediate samples.

Probe	DNA concentration [ng / $\mu$ L]	Volume [mL]	absolute DNA mass [ $\mu$ g]
I7	120.0	2.75	330
P7	61.5	1.3	80
P8 <sub>i</sub>	47.2	5	236
P8 <sub>ii</sub>	1.1	5	5.5
P8 <sub>iii</sub>	0.6	5	3
P8 <sub>iv</sub>	0.1	5	0.5
P9	1.0	5	5
P10	5.1	0.1	0.5

These data allowed to map the distribution of the DNA material (in the following indicated as red numbers) initially applied to the column in the form of I7. As for step 7 (Figure 8), 250  $\mu$ g of DNA remain in the column, while 80  $\mu$ g pass through.

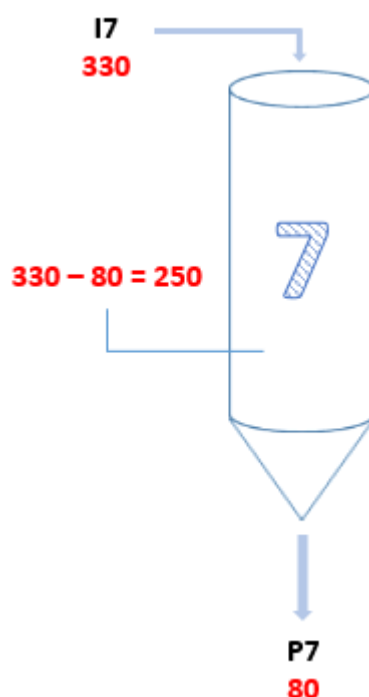


Figure 8 Distribution of DNA material in step 7. Red values carry the dimension of  $\mu$ g.

Of the 250  $\mu$ g of DNA remaining in the column, 245  $\mu$ g were washed away in step 8 as seen in Figure 9.

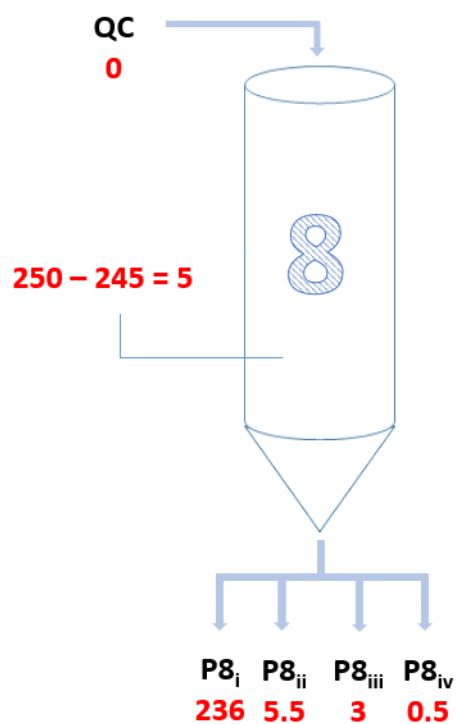


Figure 9 Distribution of DNA material in step 8. Red values carry the dimension of  $\mu\text{g}$ .

Subsequently, the elution step 9 dissolves 5  $\mu\text{g}$  DNA material from the column (Figure 10).

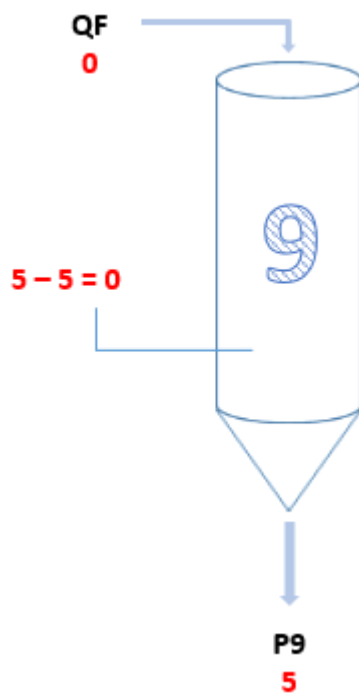


Figure 10 Distribution of DNA material in step 9. Red values carry the dimension of  $\mu\text{g}$ .

Lastly, only 0.5  $\mu\text{g}$  of initially 5  $\mu\text{g}$  DNA is yielded after precipitation and centrifugation in step 10 (Figure 11).



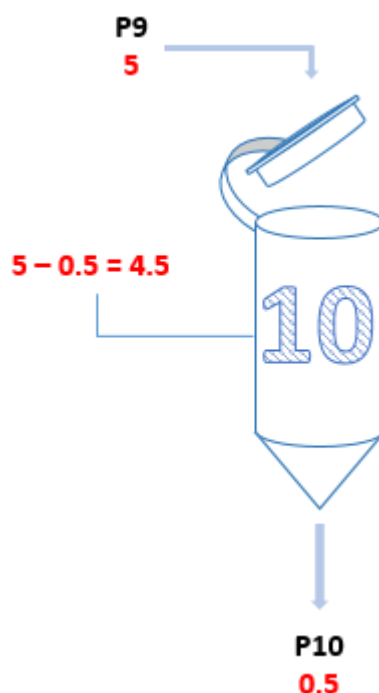


Figure 11 Distribution of DNA material in step 10. Red values carry the dimension of  $\mu\text{g}$ .

The results visualized in Figure 11 suggested that plasmids were indeed present between step 9 and 10 to an amount of 5  $\mu\text{g}$ . However, only 10 % of this mass was measured after precipitation and centrifugation. A possible explanation for the vanishing of the DNA material was that the plasmid pellet was stuck against the centrifugation tube too tightly after ultracentrifugation to be re-dissolved. Pelletized DNA would not be measurable using absorption spectroscopy. Following this assumption, the tube thought to contain the stuck, invisible DNA pellet was sonicated in short bursts. This led to an increase in DNA mass measured by several  $\mu\text{g}$ .

### 3.3.3 Optimized plasmid purification protocol

A refined protocol for plasmid purification was designed under consideration of the data acquired so far. To achieve higher total cell mass, a starting culture was incubated first and was used as inoculum for an overnight culture with a volume larger than before. Additionally, the bacterial culture tubes were sealed with perforated parafilm™ to improve aeration. Lastly, between step 10 and 11 of the medium scale plasmid purification protocol the centrifugation container was sonicated to facilitate dissolving of the DNA pellet into the buffer.

A plasmid solution acquired in this fashion was measured via absorption spectroscopy. The results are listed in Table 7.

Table 7 DNA concentration measurement after following refined protocol for plasmid purification.

Sample	260 / 280	260 / 230	DNA concentration [ $\text{ng} / \mu\text{L}$ ]	total DNA mass [ $\mu\text{g}$ ]
G	2.03	1.96	256.2	25.6

### 3.4 Testing the S30 T7 HighYield kit using VDAC

After sufficient amount of plasmid could be produced, the *in vitro* synthesis kit S30 T7 HighYield was tested. For this purpose, a positive control was used before expression of LamB was attempted. The protein voltage dependent anion channel (VDAC) was chosen as positive control, as it was reliably expressed *in vitro* with this type of IVS kit before.<sup>24</sup> VDAC has a molecular mass of 30.4 kDa. An additional negative control consisted of mere IVS reaction mix without any DNA present.

After incubation, the reaction mix was denatured through SDS treatment and loaded onto a poly-acrylamide gel. Following electrophoresis and Coomassie staining, the gel presented a band pattern as seen in Figure 12.

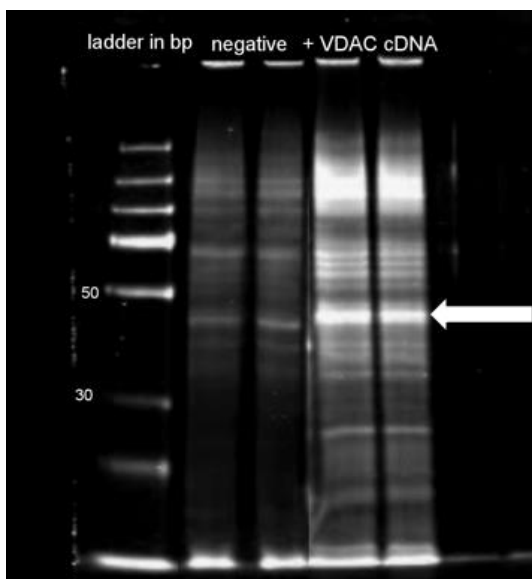


Figure 12 Scan of protein gel. Columns from left to right: Protein ladder, two times negative control, two times VDAC.

The thick band below the 50 kDa mark was thought to represent VDAC protein. The common phenomenon of 'gel-shifting'<sup>25</sup> caused this membrane protein to appear heavier than its expected mass.

Since the protein of interest, VDAC, was successfully expressed, the IVS kit was considered properly functioning.

### 3.5 IVS without purification

After characterizing and amplifying the plasmid pBSK (+) and testing the IVS kit in question, expression of LamB was attempted. The LamB carrying construct was added to the IVS reaction mix and incubation was initiated. Additionally a negative control, without any DNA added and a positive control containing DNA for a luciferase were set up.

Subsequently, the samples underwent an SDS-PAGE followed by Coomassie blue staining. The results are shown in Figure 13.

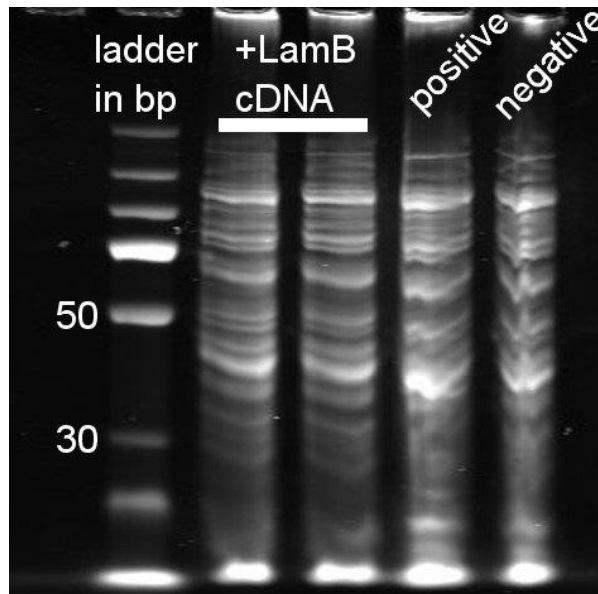


Figure 13 Coomassie staining after *in vitro* synthesis attempt of LamB without further purification of gel. Positive: contains cDNA for luciferase. Negative: no DNA was added. +Lam cDNA: two identical samples were loaded onto the gel.

No significant difference between the four columns was observed. The kit appeared to provide a strong background of numerous proteins, possibly masking the presence of potentially expressed LamB and luciferase.

### 3.6 IVS and post-synthesis purification methods

In order to reduce the background signal caused by protein components of the IVS reaction mix after Coomassie staining, three methods were applied. The first method utilised antibodies (Ab) linked to silica nanoparticles (SiNPs) to selectively bind LamB from the solution.

In a second approach, filter membranes were used to perform dialysis of the reaction mix. The cut-offs were chosen in a fashion to discard proteins larger (above 50 kDa) and smaller (below 25 kDa) than maltoporin.

In a third purification method filter membranes with a cut-off of 100 kDa were utilized to retain polymersomes, in which LamB was thought to be incorporated.

#### 3.6.1 Antibody-modified silica nano-particles

An IVS mixture was set up and supplemented with polymersomes and incubated. Antibody-modified silica nano-particles were added to the reaction mix after incubation. Anti-PEG antibodies targeted polymersomes in the solution, regardless of successful incorporation of LamB. In a secondary step, Ab against LamB specifically selected for the protein of interest.

Ab-SiNP-constructs plus potentially attached targets were isolated from the solution by centrifugation. The pH was increased to trigger detachment of anti-bodies and particles. The latter were subsequently removed through centrifugation. The supernatant underwent SDS treatment and PAGE. Resulting gels were stained with Coomassie blue dye.

#### 3.6.1.1 Purification with SiNPs (anti-PEG)

Results of purification of the IVS reaction mix via anti-PEG anti-bodies are shown in Figure 14.

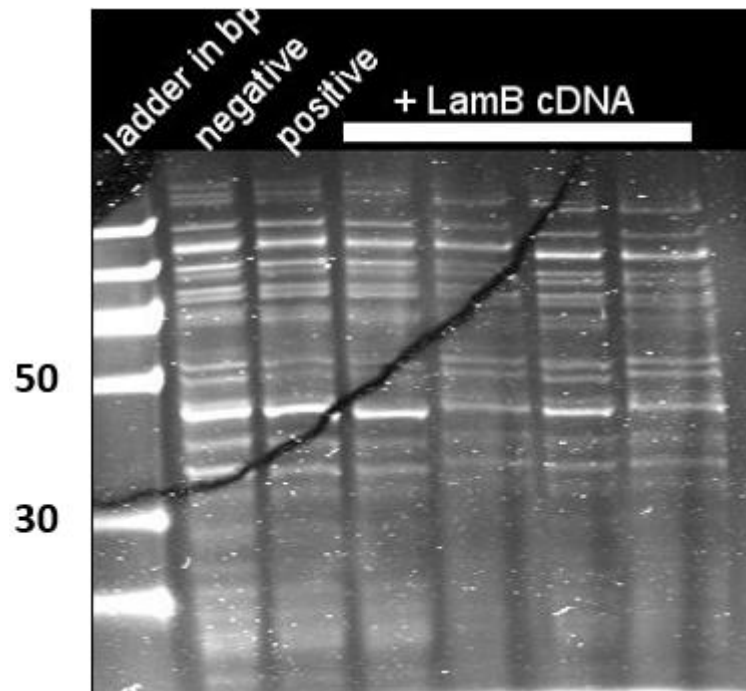


*Figure 14 Coomassie stained gel of IVS reaction mix purified with anti-PEG. Positive: contains cDNA for luciferase. Negative: no DNA was added. +LamB cDNA: IVS reaction mix volume was split in four identical samples.*

Since the batch containing luciferase DNA lacked the LamB gene, it can be regarded as another negative control. Both negative controls, as well as the four LamB samples, were still rich in background signal. A second purification step was therefore performed.

#### 3.6.1.2 Purification with SiNPs (anti-PEG + anti-Maltoporin)

After harvesting via anti-PEG, the same procedure was repeated using anti-LamB labelled nano-particles. Results of this two-step purification are presented in Figure 15.

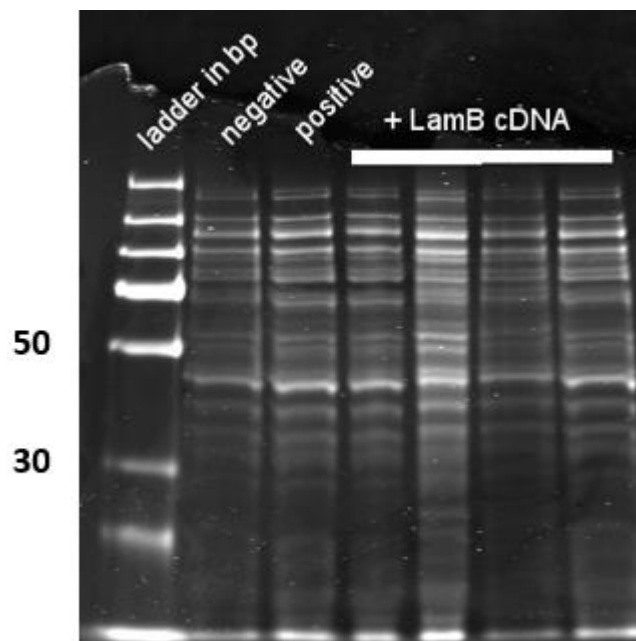


Figure 15 Coomassie stained gel of IVS reaction mix purified via anti-PEG and anti-LamB. Positive: contains cDNA for luciferase. Negative: no DNA was added. +LamB cDNA: IVS reaction mix volume was split in four identical samples.

Even after two SiNP-based purification steps, numerous protein bands appeared on the gel. In search for more efficient means of isolating potential LamB in the reaction mix, dialysis was considered.

### 3.6.2 Dialysis with 25 kDa and 50 kDa cut-offs

Protein *in vitro* synthesis batches with LamB encoding DNA and without genetic material were set up. After incubation, the reaction mixtures underwent dialysis. First, a membrane with a molecular weight cut-off of 25 kDa was used to remove solutes below that threshold. In a second dialysis step, another membrane separated molecular species above 50 kDa from the sample. The remaining protein solution was lyophilized, rehydrated and the protein concentration was then increased through evaporation via a SpeedVac® device. Aliquots of 10  $\mu$ L were treated with SDS before they underwent PAGE. The Coomassie stained polyacrylamide gel is depicted in Figure 16.

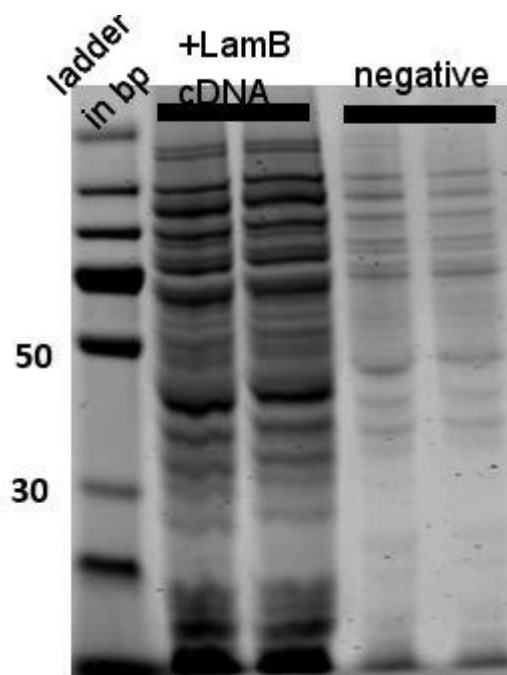


Figure 16 Coomassie stained gel after dialysis with 25 kDa and 50 kDa membranes. Negative: no DNA was added to this IVS reaction mix. +LamB cDNA: The IVS reaction mix volume was split into two identical samples.

A prominent band appeared in the region of interest at around 47 kDa in the LamB columns. However, the difference between the LamB sample and the negative control in overall intensity did not allow for quantitative comparison of the signals. The complex sample preparation, due to repeated transfer from one vessel to another, may cause material losses and consequent inconsistencies on the gel. A new dialysis system was therefore tested in the following.

### 3.6.3 Dialysis with 100 kDa cut-off

A new dialysis method was developed in order to reduce material losses through multiple change of vessel. Utilising a membrane with a molecular weight cut-off of 100 kDa, the IVS reaction mixture is dialysed after incubation. To prevent LamB, whose molecular weight is 47 kDa, from being washed away, polymersomes were added. The protein of interest was believed to be incorporated in or at least associated with the polymersomes, therefore forming a structure above 100 kDa.

However, for this purification method to efficiently work, polymersomes must withstand the incubation process as well as the dialysis environment. To investigate their survivability, samples of vesicles were observed microscopically before and after IVS incubation.

#### 3.6.3.1 Polymersome synthesis for electron microscopy

Two methods of polymersome synthesis from monomers were tested, solvent exchange and polymer film rehydration. Subsequent observation under the light microscope was used to decide for a method of choice. Polymer film rehydration proofed to yield more polymersomes, while also maintaining a more narrow size distribution.

### 3.6.3.2 Transmission electron microscopy (TEM) imaging

A new LamB-IVS batch was set up. The batch was supplemented with BD<sub>22/13</sub> polymersomes, synthesised through polymer film rehydration. After incubation, overnight dialysis against MilliQ water was carried out utilizing a 100 kDa molecular weight cut-off membrane. The *in vitro* synthesis mixture was then transferred onto a copper grid and analysed under a transmission electron microscope. A representative image acquired in this way is depicted in Figure 17.

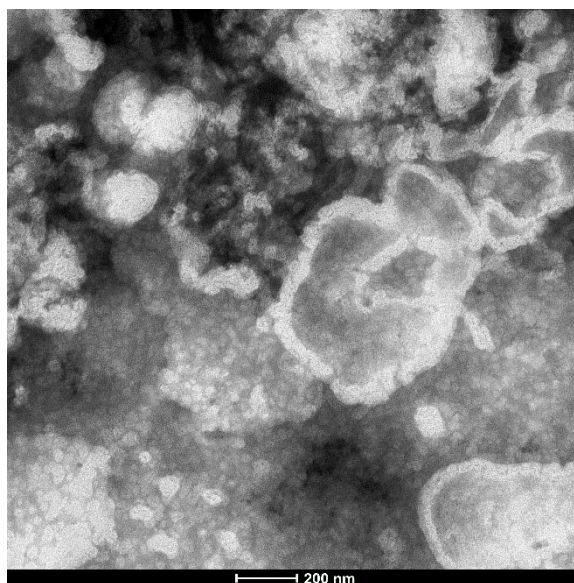


Figure 17 Transmission electron microscope image of IVS reaction mix with polymersomes after dialysis. Scale bar 200 nm.

No polymersomes were visible on the grid, but collapsed structures. Since polymersomes were present before their solution was added to the IVS reaction mix, polymersomes disappeared either during incubation, dialysis, sample preparation or TEM analysis in high vacuum. To further investigate the specific time point of their collapsing, confocal laser microscopy (CLM) instead of transmission electron microscopy was used. CLM does not require any sample preparation and does not operate under high vacuum. Sample preparation and vacuum could thereby be eliminated as source of destruction. A potential collapsing of the polymersomes during IVS incubation or dialysis could therefore be more easily investigated.

### 3.6.3.3 Electroformation of polymersomes for CLM analysis

For better visualisation, giant unilaminar vesicles (GUVs) were produced. Electroformation was chosen as desired method of synthesis, since it provides an established technique in our working group for the production of GUVs. Polymersomes crafted from BD<sub>12/9</sub> with 1 % fluorescent-labelled phosphocoline of a size of 5 – 60  $\mu\text{m}$  were provided from a member of this working group. Two species of polymersomes were tested. One filled with 150 mM sucrose and one with MilliQ water.

### 3.6.3.4 Confocal laser microscopy

Two IVS batches were set up and supplemented with fluorescent polymersomes (once filled with sucrose, once with MilliQ water) synthesised through electroformation. The reaction mix was then dialysed against a sucrose solution and MilliQ water respectively. An aliquot of the reaction mix was loaded on a glass slide and observed under the microscope. The fluorescent



sucrose-filled polymersomes were clearly visible as seen in Figure 18. Water-filled polymersomes provided no fluorescent signal.

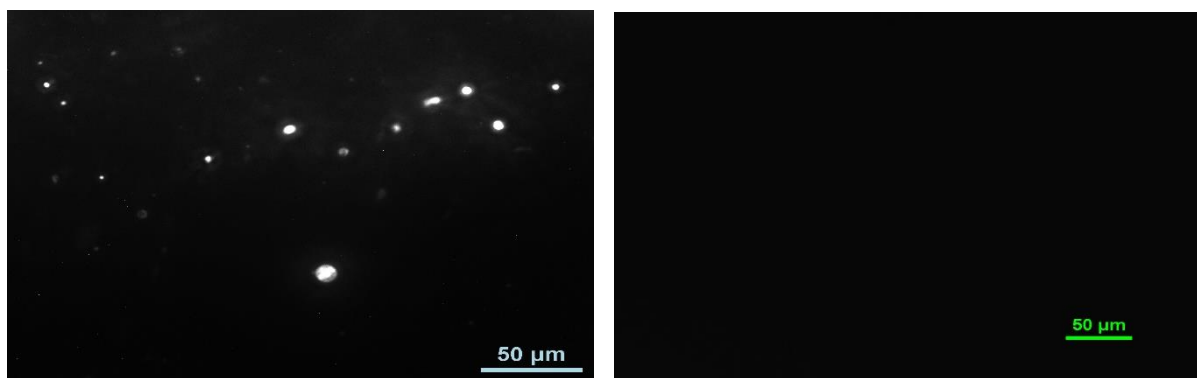


Figure 18 Left: Several polymersomes are visible after IVS incubation and dialysis under the fluorescent microscope. Right: No fluorescent signal is obtained in case of polymersomes filled with water.

As polymersomes filled with 150 mM sucrose solution withstood the post-IVS dialysis, polymersomes in the following *in vitro* synthesis batches were also prepared in this fashion. It was assumed that the sucrose solution on the inside reduced the difference in osmotic pressure across the polymersome membrane.

### 3.7 IVS with optimized purification method

Two IVS reaction batches were set up and were supplemented with polymersomes, which contained a 150 mM sucrose solution on the inside. The first sample contained the LamB gene, whereas the second one lacked any DNA material, thereby serving as a negative control. After incubation, dialysis against a 150 mM sucrose solution was carried out overnight. Aliquots of both samples were treated with SDS and subsequently underwent PAGE. The resulting gel was Coomassie stained and is depicted in Figure 19.



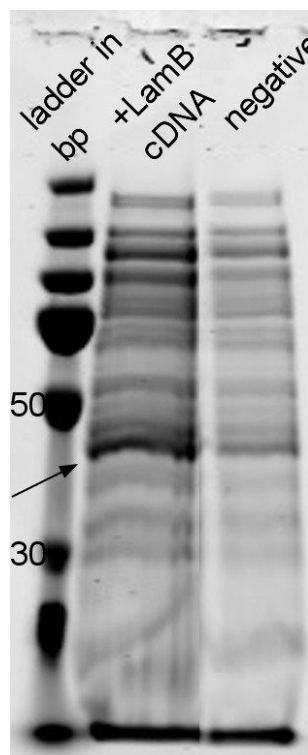


Figure 19 Commassie stained protein gel after optimized purification. A dominant band below the 50 kDa mark is visible (black arrow). Negative: no cDNA was added to the IVS reaction mix.

Maltoporin, having a molecular weight of 47 kDa, was expected to cause a band just below the 50 kDa mark. This, however, was the case not only for the first column, where LamB cDNA was added, but also in the negative control (third lane). Although the sample lane (second lane) has a higher overall intensity than the third one, the second band still appeared to be more dominant than the one on the negative control.

It was therefore assumed that an IVS kit component, which showed a comparable PAGE migration behaviour as maltoporin, was masking LamB. This unknown protein will be referred to as “LamB mimicking protein” (LMP) in this thesis. In the following, steps were undertaken to separate the protein band of LamB from the band LMP.

### 3.8 Separation LamB and LMP through low voltage SDS-PAGE

*In vitro* synthesis mixtures were set up, supplemented with polymersomes and incubated. Subsequently, dialysis was carried out, before samples were transferred on a poly-acrylamide gel. In order to separate the protein bands in question, electrophoresis was run with a reduced voltage of just 100 V. The slower and longer migration was believed to give rise to more sharply defined bands. The resulting gel after Coomassie staining is depicted in Figure 20.

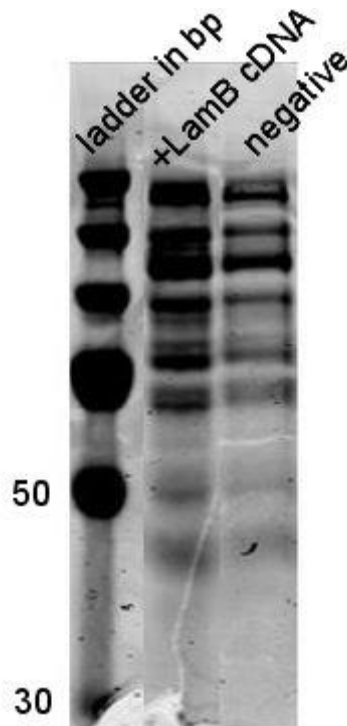


Figure 20 Coomassie stained gel after electrophoresis at 100 V. Negative: no cDNA was added to the IVS reaction mix.

Reduction of voltage did not lead to sharper bands, but caused the opposite effect. Bands (including those of the protein ruler) appeared broader and with undefined borders. This method therefore proved not fruitful in separating LamB and LMP and was discarded.

### 3.9 Separation of LamB and LMP through fluorescent amino acids

In a second attempt to visually separate the two bands of LMP and LamB, the IVS reaction mixture was supplemented with fluorescently tagged L-lysine. Therefore, proteins translated during the *in vitro* synthesis would partially incorporate the modified lysine. Proteins which were present in the IVS-kit all along would not gain the ability to fluoresce. The band caused by LamB should therefore be clearly distinguishable. After incubation, SDS-PAGE was carried out. The resulting gel was excited with UV-light to visualize fluorescent bands and is shown Figure 21.

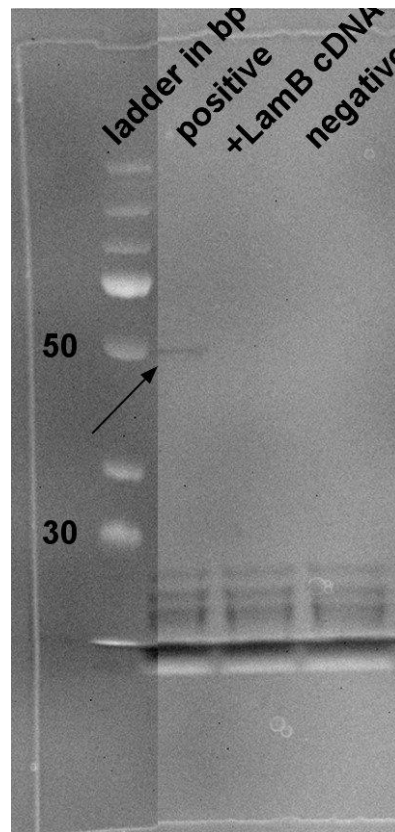


Figure 21 Resulting gel from IVS with addition of fluorescent amino acids. Band in positive control is indicated by a black arrow. Positive: contains cDNA for CD4. Negative: no DNA was added.

The positive control, CD4 expressed with a wheat germ IVS kit, produced a band close to the 50 kDa mark (Figure 21, black arrow). However, no fluorescence was detected in case of the LamB sample. This was taken as indication that maltoporin was not expressed.

### 3.10 Mass spectrometry

Former experiments suggested that the band thought to contain LamB and LMP was indeed lacking LamB. To further characterize the band in question, protein sequencing through mass spectrometry was carried out. An *in vitro* synthesis batch was set up and LamB encoding plasmids were added. After incubation, the gel was stained using Coomassie dye and subsequently washed overnight. It was then handed over to the Department of Chemistry (University of Natural Resources and Life Sciences, Vienna), where the band in question was analysed via mass spectroscopy. The resulting list of detected proteins is given in **Fehler! Verweisquelle konnte nicht gefunden werden..**

Table 8 List of proteins detected via mass spectroscopy with corresponding MASCOT score. Only the first ten entries were listed here. The full list can be found under Supplemental Information.

protein	MASCOT Score
Elongation Factor Tu 2 ( <i>E. Coli</i> )	1985.1
Enolase ( <i>E. Coli</i> )	1149.2
Transcription Termination Factor Rho ( <i>E. Coli</i> )	779.9
Maltose-binding periplasmic protein ( <i>E. Coli</i> )	709.2
Phosphoglycerate Kinase ( <i>E. Coli</i> )	673.3
Isocitrate Dehydrogenase ( <i>E. Coli</i> )	665.6
Cysteine Desulfurase ( <i>E. Coli</i> )	644.1
Adenylosuccinate Synthetase ( <i>E. Coli</i> )	585.5
Succinyl-CoA Ligase Subunit Beta ( <i>E. Coli</i> )	572.2
6-phosphogluconate Dehydrogenase ( <i>E. Coli</i> )	496.2

Maltoporin not being detected through this sequencing method was taken as another indication that the protein of interest was not being translated.

### 3.11 DNA sequencing analysis of pBSK(+)

A possible reason for the failed *in vitro* expression of LamB was believed to be a dysfunction of the plasmid used. The DNA sequence of the pBSK(+) vector was therefore investigated. Common features (promoters and open reading frames) were detected and visualized using SnapGene Viewer. The results are shown in Figure 22.

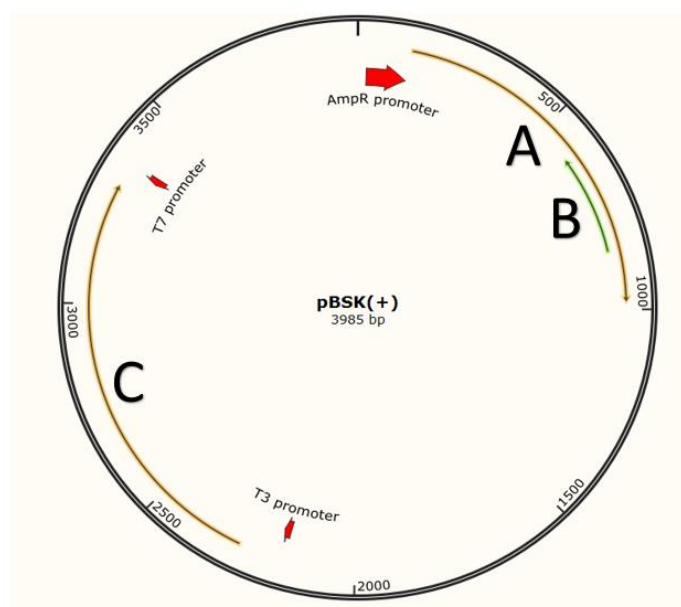


Figure 22 SnapGene Viewer maps common features on pBSK(+): three promoter sequences (red arrows) and three open reading frames (orange and green arrows).

The software detected three promoters (AmpR promoter: 24-128, T3: 2171-2189, T7: 3360-3342) and three ORFs (A: 129-861, B: 859-593 and C: 2279-3304). ORF A appears to be under control of the AmpR promoter. ORF B seems to lack an appropriate promoter. Lastly, ORF C is positioned downstream of promoter T3, but with a spacer of 90 bp. The same ORF also lies close to the T7 promoter, which, however, is located at the 3' end of the frame.

Basic Local Alignment Search Tool (BLAST) was used to assess the detected ORFs' DNA sequences. Frame A showed 100 % identity to class A broad-spectrum beta-lactamase TEM-116 (Sequence ID: WP\_000027050.1). Since resistance to the antibiotic ampicillin is often mediated by beta-lactamases<sup>26</sup>, this ORF was assumed to be responsible for ampicillin resistance.

Frame B did not translate into an independent protein.

Frame C was compared with the reverse-transcribed sequence of LamB, that was submitted to the manufacturer of pBSK(+) (Figure 26). BLAST results indicated an identity of 84 % between both sequences, but revealed ORF C to be truncated with a sequence coverage of only 76 % (Figure 23).

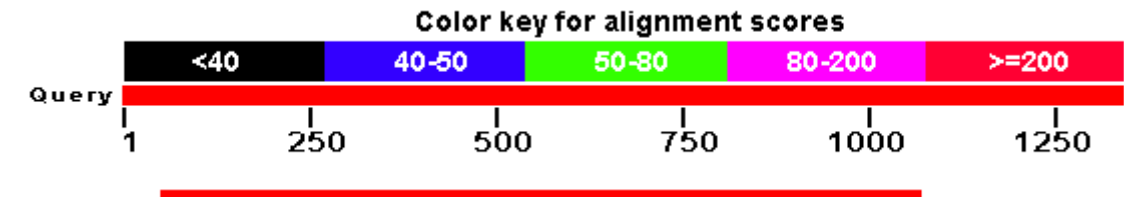


Figure 23 Results of BLAST analysis of desired plasmid insert (query, thick red line), and ORF C (subject, thin red line).

Comparison of the respective amino acid sequences yielded 100 % identity, and a sequence coverage of 82 % (Figure 24).

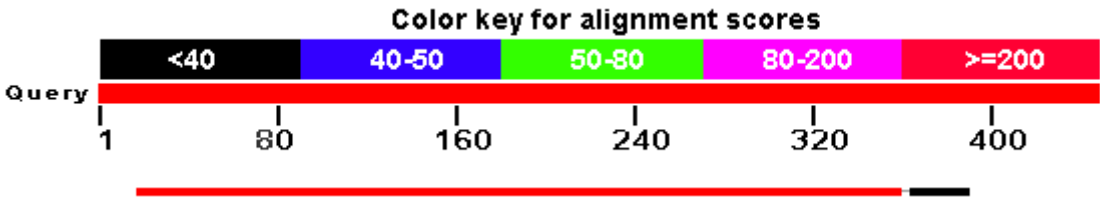


Figure 24 Comparison of amino acid sequences of the desired plasmid insert (query, thick red line), and ORF C (subject, thin red line).

The differences between the identities of the DNA sequences and amino acid sequences was most likely due to synonymous codon exchange performed by the manufacturer as host specific codon optimisation.

The defective DNA sequence (i.e. miss-positioned promotor and truncated cDNA) can be identified as the main reason for the failed expression of LamB.

## 4 Material and Methods

### 4.1 Designing and ordering pBSK(+)

The plasmid pBSK(+) Simple-Amp from Biomatik was chosen as expression vector. The amino acid sequence of *Shigella sonnei*'s maltoporin was provided by NCBI's protein database (Reference Sequence: WP\_052994967.1) and is listed below in Figure 25.

```
mmitlrklpl avavaagvms aqamavdfhg yarsgigwtg sggeqqcfqt  
tgaqskyrlg necetyaelk lgqevwkegd ksfyfdtnva ysvaqqndwe  
atdpafrean vqgknliewl pgstiwagkr fyqrhdvhmi dfyywdisgp  
gaglenidvg fgklslaatr sseaggsssf asnniydytn etandvfdvr  
laqmeinpgg tlelgvdygr anlrdnyrlv dgaskdgwlf taehtqsvlk  
gfnkfvvqya tdsmtsqqkg lsqsgsvafd nekfayninn nghmlrildh  
gaismgdnwd mmyvvgmyqdi nwdndngtkw wtvgirpmyk wtpimstvme  
igydnvesqr tgdknnqyki tlaqqwqagd siwsrpairv fatyakwdek  
wgydyngdsk vnpnygkavp adfnggsfgr ggsdewtfga qmeiww
```

Figure 25 Amino sequence of LamB from *Shigella sonnei*.

The sequence above was reverse-translated into nucleotide format using the online software Sequence Manipulation Suite: Reverse Translate.<sup>27</sup> Each amino acid was converted into its most likely codon in *E. Coli*. The resulting nucleotide sequence is listed in Figure 26.

```
5'atgatgatta ccctgcgcaa actgccgctg gcggtggcgg tggcggcggg cgtgatgagc  
gcgcaggcga tggcgggtga ttttcatggc tatgcgcgca gcggcattgg ctggaccggc agcggcggcg  
aacagcagtg ctttcagacc accggcgcgc agagcaaata tcgcctgggc aacgaatgcy aaacctatgc  
ggaactgaaa ctgggccagg aagtgtggaa agaaggcgat aaaagctttt attttgatac caacgtggcg  
tatagcgtgg cgcagcagaa cgattgggaa gcgaccgatc cggcgtttcg cgaagcgaac gtgcagggca  
aaaacctgat tgaatggctg ccgggcagca ccatttgggc gggcaaacgc ttttatcagc gccatgatgt  
gcatatgatt gatttttatt attgggatat tagcggcccg ggcgcgggccc tggaaaacat tgatgtgggc  
tttggcaaac tgagcctggc ggcgaccgc agcagcgaag cgggcggcag cagcagcttt gcgagcaaca  
acatttatga ttataccaac gaaaccgcga acgatgtgtt tgatgtgcgc ctggcgcaga tggaaattaa  
cccgggcggc accctggaac tgggcgtgga ttatggccgc gcgaacctgc gcgataacta tcgcctggtg  
gatggcgcgga gcaaagatgg ctggctggtt accgcggaac ataccagag cgtgctgaaa ggctttaaca  
aatttgtggt gcagtatgcy accgatagca tgaccagcca gggcaaaggc ctgagccagg gcagcggcgt  
ggcgtttgat aacgaaaaat ttgcgtataa cattaacaac aacggccata tgctgcgcac tctggatcat  
ggcgcgatta gcatggcgga taactgggat atgatgtatg tgggcatgta tcaggatatt aactgggata  
acgataacgg caccaaatgg tggaccgtgg gcattcgccc gatgtataaa tggacccgga ttatgagcac  
cgtgatggaa attggctatg ataacgtgga aagccagcgc accggcgata aaaacaacca gtataaaatt  
accctggcgc agcagtggca ggcgggcgat agcatttggga gccgcccggc gattcgcgtg tttgcgacct  
atgcgaaatg ggatgaaaaa tggggctatg attataacgg cgatagcaaa gtgaaccgga actatggcaa  
agcggtgccg gcgattttta acggcggcag ctttggccgc ggcggcagcg atgaatggac ctttggcgcg
```

Figure 26 Reverse-translated nucleotide sequence of *Shigella sonnei*'s LamB.

The sequence of Figure 26 was forwarded to the provider and the option to further optimize the DNA for expression in *E. Coli* was chosen. Cloning the insert into the MCS was carried out by the provider Biomatik.

## 4.2 DNase digest of pBSK(+)

To characterize the construct, Thermo Fisher's FastDigest kit (Cat. No. ER0501) was used. 2  $\mu$ L plasmid solution containing 500 ng of the pBSK(+) vector, 2  $\mu$ L enzyme solution (HindIII), 2  $\mu$ L of FastDigest Green Buffer and 14  $\mu$ L Milli-Q water were combined. After an incubation of 45 minutes at 37° C, the DNA fragments were transferred onto an agarose gel and gel electrophoresis was carried out. Bands were subsequently visualised using UV-Light ( $\lambda = 366$  nm).

## 4.3 Primer design for PCR

Two primers targeting the cDNA of LamB were designed. The forward primer was complementary to nucleotides 2213 - 2238 of the coding strand (26 bases long). The backward primer was complementary to nucleotides 3372 - 3402 of the non-coding strand (26 bases long). The primers' sequences and targets are listed in Table 9.

Table 9 Targeted cDNA sequences and corresponding primers

	targeted sequence on cDNA	primer sequence	primer sequence 5' – 3'
<b>Forward</b>	5' GTGAGCGGATAACAATTTACACA GG 3'	3' GTGAGCGGATAACAATTTACACA GG 5'	5' CCTGTGTGAAATTGTTATCCGCTCA C 3'
<b>Reversed</b>	3' AGCCGATACTATTACACCTTAGAGT C 5'	5' CTGAGATTCCACATTATCATAGCCG A 3'	5' TCGGCTATGATAATGTGGAATCTCA G 3'

Annealing temperature and melting points were calculated using Thermo Fisher's online calculator<sup>28</sup> and listed in Table 10 and Table 11. Table 11 Calculated annealing temperature for the Taq polymerase..

Table 10 Melting temperatures of the two primers.

	melting temperature
<b>Forward</b>	59.8° C
<b>Reversed</b>	57.6° C

Table 11 Calculated annealing temperature for the Taq polymerase.

<b>annealing temperature Taq polymerase</b>	52.6° C
---	---------

## 4.4 PCR

Polymerase chain reaction was carried out on a Primus 96 Advanced by the manufacturer Peqlab. Nucleotides, PCR premix, Taq polymerase was provided by Sigma (Taq DNA Polymerase from *Thermus aquaticus*, Lot. SLBM4174, Cat. D1086-250UN). Nucleotide solutions of this kit were diluted 1:10 in MilliQ water before usage. A reaction mix consisted of the components listed in Table 12.

Table 12 PCR mix composition.

PCR 10 x buffer	5 µL
dATP 1:10	0.5 µL
dGTP 1:10	0.5 µL
dCTP 1:10	0.5 µL
dTTP 1:10	0.5 µL
Primer forward	3 µL
Primer reversed	2.6 µL
Taq polymerase	0.5 µL
pBSK(+)	1 µL
MilliQ water	35.5 µL

PCR conditions were set as listed in Table 13.

Table 13 PCR conditions.

preheat	99° C	} 30 loops
denaturation	94° C for 1 min	
annealing	52.6° C for 2 min	
extension	70° C for 1.5 min	
finalising	60° C for 5 min	

#### 4.5 Transformation of *E. coli*

*E. coli* strain TOP10 was chosen as amplification host to replicate pBSK(+) Simple-Amp carrying Lamb. The transformation kit One Shot TOP10 Chemically Competent *E. coli* was purchased from Invitrogen (Cat. No. C404010). Transformation was carried out according to the manufacturer's protocol with 100 ng plasmid material.

The heat shock-treated bacteria were transferred in equal parts unto three agar plates. Each gel was cast from 20 mL of LB agar solution (Table 14) and supplemented with 2 mg ampicillin.

Table 14 Composition of agar gel for plate cultures.

LB-Agar	10 g / L
LB Broth	10 g / L
Maltose	5 g / L
MilliQ water	to a volume of 1 L

#### 4.6 Liquid culture

Successfully transformed cells served as inoculum for liquid culture. Lysogeny broth<sup>29</sup> with 100 µg / mL ampicillin served as medium (Table 15). One colony per vial of liquid culture was added. Incubation was carried out overnight at 37° C at 40 rpm in a sealed 20 mL tube.

Table 15 Composition of lysogeny broth.

Yeast extract	5 g / L
Trypton	10 g / L
NaCl	5 g / L
Maltose	5 g / L



#### 4.7 Plasmid purification

Plasmids were purified using QUIAGEN's Plasmid Mini Kit (25) ("Miniprep") (Cat. No 12123) for volumes below 100 mL culture volume. Higher volumes were processed via QUIAGEN's Plasmid Midi Kit (25) ("Midiprep") (Cat. No. 12143).

#### 4.8 Absorption measurement

DNA concentrations were evaluated using NanoDrop's spectrophotometer ND-1000 coupled with the NanoDrop ND-1000 V3.5.2 software. The device was loaded with volumes of 3  $\mu$ L. Blank values were acquired from measuring MilliQ water droplets.

From the absorption at 260 nm wavelength, the DNA concentration is calculated via Lambert-Beer's law. Ratios between absorption at 260 nm and 230 nm, as well as 260 nm and 230 nm were noted respectively.

Three aliquots of each sample were measured. The mean value of these three measurements was calculated and listed as result.

#### 4.9 Vacuum assisted concentration

Vacuum assisted concentration was carried out with a SAVANT ISS110 SpeedVac concentrator from Thermo Scientific with drying rate set to "high". Liquid samples were transferred into 2 mL Eppendorf tubes and placed in the rotor.

#### 4.10 Refined liquid culture and plasmid purification

This improved protocol was based on the protocol found in chapter 4.6, Table 5. Unless pointed out differently, the same methods and materials apply. A 5 mL starting culture was incubated for 3h. It then served as inoculum for a three times 33 mL overnight culture (1.6 mL inoculum per tube). Incubation tubes were sealed with perforated parafilm™ to enhance aeration.

After 16 hours of incubation, the culture was processed via MidiPrep. The bacterial pellets resulting from step 2 were united and redissolved in 4 mL resuspension buffer. After step 10 of the manufacturer's protocol, the centrifugation tube, now filled with TAE buffer, was sonicated for five times one second.

#### 4.11 Testing the IVS kit

For all *in vitro* protein expression experiments, Promegas S30 T7 High-Yield Protein Expression System was used (Cat. L1110). To test the proper functionality of the IVS kit, a test run with two variants of the gene voltage-dependent anion channel (VDAC) is performed. Three IVS reaction mixes were set up as seen in Table 16.

Table 16 IVS reaction mix composition for VDAC production.

sample	plasmid [ng]	amino acid mix [μL]	S30 premix [μL]	T7 S30 extract [μL]	MilliQ water [μL]
H	0	5	20	15	10
I	1000	5	20	15	6
J	2000	5	20	15	3

Incubation was carried out at 37° C for two hours under continuous shaking at 300 rpm. The expression was terminated by placing the test tube on ice.

#### 4.12 SDS-Page

All sodium dodecyl sulfate polyacrylamide gel electrophoresis (SDS-PAGE) assays were carried out with Thermo Fisher's NuPAGE Electrophoresis System. This includes pre-cast gels (REF: NP0301BOX), NuPAGE LDS Sample Buffer (REF: NP0007), NuPAGE Reducing Agent (REF: NP009), NuPAGE MOPS Running Buffer (REF: NP001) and Novex Mini-Cell (Serial No: 110501-0612). The power source was BIO-RAD PowerPac 300 (Serial No. 283BR00986). A voltage of 200 V was applied unless stated differently.<sup>30</sup>

#### 4.13 Protein staining

SDS-Page gels were rinsed three times with 40 mL MilliQ water. Thereafter, 20 mL of the dye SimplyBlue SafeStain (Cat. No. LC6060) by Invitrogen were applied and gels were incubated for one hour. The staining agent was discarded and the gel was washed with MilliQ water for one hour.

#### 4.14 DNA gel and electrophoresis set-up

For DNA gel electrophoresis, 1 % Agarose gels are casted as described in Table 17. Agarose was acquired from QIAGEN (Mat.No. 1062631, Lot. 136258626). SYBR Safe DNA Gel Stain was purchased from Invitrogen (Cat. S33102, Lot. 1459613).

Table 17 Composition of DNA gel.

Agarose	0.35 g
MilliQ water	35 mL
SYBR Safe DNA Gel Stain	3.5 μL

After uniting all ingredients, the mix was stirred manually until all powder was dispersed. The liquid was brought to boiling in a microwave and was subsequently poured into its cast. After 30 minutes of cooling, the gel had hardened and was ready to be loaded with samples.

The gel was placed in a scaffold and submerged in TAE buffer. Electrophoresis was performed under a voltage of 80 V for 30 minutes.

BIO-RAD's MINI-SUB CELL GT (Serial No. 712BR 19770) was used as scaffold. The power source was BIO-RAD's PowerPac 300 (Serial No. 283BR00986). UltraPure DNA Typing Grade TAE Buffer (Cat. 24710-030, Lot. 1782268) was bought from Invitrogen.

DNA bands were then visualized under UV-light of peqlab's BIO-VISION-3026 WL/26MX (Serial No. 08 200607), supported by the software VisionCapt (Version 15.01 for Windows) by Vilber Lourmat.

#### 4.15 IVS without purification

*In vitro* protein synthesis of LamB was attempted via Promega's S30 T7 High-Yield Protein Expression System, by adding pBSK(+) as DNA template.

Additionally, a negative and a positive control were used. The negative control contained no DNA, whereas in the positive control *Renilla* luciferase encoding DNA, provided by the manufacturer, served as template. This luciferase has a molecular weight of 37 kDa, but appears on SDS-PAGE gels at a mass of about 33 kDa, as stated by the manufacturer.

Preparation and incubation was carried out as recommended in the manufacturer's manual. Compositions of the individual IVS batches are listed in Table 18.

Table 18 Composition of IVS batches; 38.1: negative control, 38.2: positive control, 38.5 and 38.6 contained the *LamB* gene.

sample	plasmid [ng]	amino acid mix [μL]	S30 premix [μL]	T7 S30 extract [μL]	MilliQ water [μL]	polymersome solution [μL]
38.1	0	5	20	15	10	0
38.2	2000	5	20	15	6	0
38.5	729	5	20	15	2	0
38.6	729	5	20	15	2	0

Incubation was carried out at 37° C for two hours under continuous shaking at 300 rpm. The expression was then stopped by placing the test tube on ice.

#### 4.16 Antibodies (Abs)

Anti-maltoporin antibodies were purchased from biorbyt (Cat. No. orb159196). The IgG antibodies were produced in a rabbit host system. They were targeted against the immunogen KLH conjugated synthetic peptide derived from human maltoporin. Abs were stored as 0.5 mg / mL stock solution in 10 mM PBS, pH 7.4 with 10 mg / mL BSA, 0.03% Proclin 300 and 25% glycerol at -20° C.

Monoclonal anti-poly-ethylene-glycol antibodies derived from a rabbit host were purchased from ABCAM (Cat. No. ab51257).

#### 4.17 Immuno-functionalised silica nanoparticles

Silica nanoparticles (SiNPs) were synthesized via the Stöber-process<sup>31</sup> yielding a SiNP-solution of 185 μg / μL with an average particle diameter of 467 nm.

SiNPs-Ab-conjugates were formed by EDC/NHS coupling chemistry. Two different species of antibodies were used: anti-maltoporin and anti-PEG. Two times 33  $\mu\text{L}$  SiNP-solution were amino-functionalized. This volume contained 6.1 mg SiNPs or  $1.04 * 10^{-13}$  mol as can be seen in Equation 1 and Equation 2.

Equation 1

$$33 \mu\text{L} * 185 \frac{\mu\text{g}}{\mu\text{L}} = 6105 \mu\text{g} \triangleq 6.11 \text{ mg}$$

Equation 2

$$\frac{6.11 \text{ mg}}{Mw} = 1.04 * 10^{-13} \text{ mol}$$

Each particle was estimated to carry roughly 1000 carboxyl groups. The total amount of carboxyl groups in 33  $\mu\text{L}$  solution is therefore given by Equation 3.

Equation 3

$$1.04 * 10^{-13} \text{ mol} * 1000 \approx 10^{-10} \text{ mol}$$

1-Ethyl-3-(3-dimethylaminopropyl)carbodiimid (EDC) and *N*-hydroxysuccinid (NHS) were added at a tenfold molar excess.

Table 19 Molecular weights of EDC and NHS.

	molecular weight [g / mol]
<b>EDC</b>	191.15
<b>NHS</b>	115.0

Equation 4

$$\text{EDC: } 191.15 \frac{\text{g}}{\text{mol}} * 10 * 10^{-10} \text{ mol} = 19.1 * 10^{-8} \text{ g} \triangleq 0.19 \mu\text{g}$$

Equation 5

$$\text{NHS: } 115.0 \frac{\text{g}}{\text{mol}} * 10 * 10^{-10} \text{ mol} = 11.5 * 10^{-8} \text{ g} \triangleq 0.12 \mu\text{g}$$

Amino functionalization was carried out by mixing EDC, NHS and SiNPs in 1 mL MilliQ water (Table 20), followed by 30 minutes of incubation at 25° C.

Table 20 EDC, NHS and SiNPs masses and amounts of substance.

Component	Mass [ $\mu\text{g}$ ]	Amount of substance [mol]
<b>EDC</b>	0.19	$19.1 * 10^{-8}$
<b>NHS</b>	0.12	$11.5 * 10^{-8}$
<b>SiNPs</b>	6110	$1.04 * 10^{-13}$

Subsequently, the now functionalized particles were spun down using a table centrifuge (1700 x g for 5 minutes). The supernatant was discarded and the pellet re-suspended in 1 mL MilliQ water under sonication. These steps were repeated twice. The SiNPs solution was then divided into two equal volumes.

The two batches were both diluted in 1 mL PBS and supplemented with the respective antibody (Table 21). Ab were added in 1000-fold molar excess in respect to the amount of SiNPs (Equation 6 to Equation 10). Coupling reaction followed over night at 25° C while being shaken at 300 rpm. The Ab-modified particles were three times washed with PBS and stored in 100

$\mu\text{L}$  PBS at 4° C the following day. These solutions are being referred to as “anti-LamB-SiNP stock solution” and “anti-PEG-SiNP stock solution” in the following.

Equation 6

$$N_{\text{SiNPs}} * 1000 = N_{\text{AB}}$$

Equation 7

$$1.04 * 10^{-13} \text{ mol} * 1000 = 1.04 * 10^{-10} \text{ mol}$$

Equation 8

$$V_{\text{AB,stock}} = N_{\text{AB}} * M_{\text{AB}} * \frac{1}{\rho_{\text{AB,stock}}}$$

Equation 9

$$\text{Anti - LamB: } V_{\text{AB,stock}} = 1.04 * 10^{-10} \text{ mol} * 150 \frac{\text{g}}{\text{mol}} * \frac{1}{0.5 \frac{\text{g}}{\text{L}}} = 3 * 10^{-8} \text{ L} \triangleq 0.03 \mu\text{L}$$

Equation 10

$$\text{Anti - PEG: } V_{\text{AB,stock}} = 1.04 * 10^{-10} \text{ mole} * 150 \frac{\text{g}}{\text{mol}} * \frac{1}{0.86 \frac{\text{g}}{\text{L}}} = 1.8 * 10^{-8} \text{ L} \triangleq 0.018 \mu\text{L}$$

Table 21 Volume of Ab solution added to activated SiNPs.

Name of batch	Volume of Ab-stock solution added [μL]
anti-LamB	0.03
anti-PEG	0.018

#### 4.18 Purification with SiNPs (anti PEG)

Six batches of IVS reaction mix were set up as seen in Table 22. Four identical ones (M to P) each contained DNA encoding for LamB. A negative control (K) was lacking DNA, while a positive control (L) with *Renilla* luciferase DNA was also set up.

Each batch contained 5  $\mu\text{L}$  of a 2 mg / mL aqueous solution of polymersomes. These were synthesised from the polymer BD<sub>116/9</sub> with a diameter of 200. The poly-ethylene-glycol moiety at the hydrophilic side represented the target for the antibody used later on.

Table 22 Composition of IVS mix batches for purification via SiNPs.

sample	plasmid [ng]	amino acid mix [μL]	S30 premix [μL]	T7 S30 extract [μL]	MilliQ water [μL]	polymersome solution [μL]
K	0	5	20	15	10	5
L	2000	5	20	15	6	5
M	2563	5	20	15	0	5
N	2563	5	20	15	0	5
O	2563	5	20	15	0	5
P	2563	5	20	15	0	5

Incubation was carried out for two hours at 37° C, while being shaken at 300 rpm. Thereafter the batches were placed on ice to stop the expression.

Each reaction batch was supplemented with 10 µL of anti-PEG-SiNP stock solution and 440 µL PBS. These mixtures were incubated for 1 hour at 25° C and 600 rpm. Nano-particles were then harvested by centrifugation, while the supernatant was discarded. 10 µL of 10 mM NaOH solution were added to separate the Abs from their particles. After 10 minutes of incubation and sonication treatment, the SiNPs were spun down using a centrifuge (1700 x g, for 5 minutes). The supernatant was thought to contain Abs bound to the PEG chains of the polymersomes. Aliquots of 10 µL of supernatant were treated with SDS and underwent PAGE subsequently.

Additional 10 µL per batch were diluted in 980 µL PBS and supplemented with 10 µL anti-LamB stock solution. These mixtures were incubated for 1 hour at 25° C and 600 rpm. Further treatment was analogous to the one of anti-PEG-Ab described in the paragraph above.

#### 4.19 25 kDa and 50 kDa membranes

The Spectra/Por 6 Dialysis Tubing system (12 mm flat-width) from Spectrumlabs was used with two different molecular weight cut-offs: 25 kDa (Part No. 132540) and 50 kDa (Part No. 132550).

#### 4.20 100 kDa membrane

Three batches of microdialysis devices (Spectra/Por microFloat-A-Lyzer) from Spectrumlabs with three pore sizes were used: 20 kDa (Part No. F235057), 50 kDa (Part No. F235058) and 100 k (Part No. F235059).

#### 4.21 Dialysis with 25 kDa and 50 kDa membranes

Two 6 cm long pieces of 25 kDa membrane were washed in 100 mL Milli Q water for 15 minutes. One end of 25 kDa membrane was sealed with a plastic clip. The tubes were then filled with 50 µL of IVS reaction mix of a composition as seen in Table 23.

*Table 23 IVS reaction mix composition for dialysis with 25 kDa and 50 kDa membranes.*

sample	plasmid [ng]	amino acid mix [µL]	S30 premix [µL]	T7 S30 extract [µL]	MilliQ water [µL]
Q	0	5	20	15	10
R	2562	5	20	15	0

The negative control (Q), as well as the sample containing LamB cDNA (R) were each pipetted into an individual tube. A second clip was used to seal off the membrane. Each sample was submerged in 100 mL MilliQ water and put on a shaker. Over the course of 4 h the dialysate was replaced by fresh MilliQ water three times.

The tube was subsequently re-opened by removing one clip. The content was transferred into a 50 kDa membrane, which was prepared and handled as was the 25 kDa membrane before.

Dialysis was carried out for 18 h. The dialysate was transferred into a round-bottom flask and lyophilised at  $-20^{\circ}\text{C}$  and 0.060 mbar. The dried contents were re-dissolved in 2 mL MilliQ water, and subsequently concentrated via a SpeedVac concentrator.

#### 4.22 Polymersome synthesis

Polymersomes were synthesized from the diblock copolymer poly-(buta-1,3-diene)-poly(ethylene oxide) ( $[\text{PBD}]_x\text{-}[\text{PEO}]_y$ ), whose structure is seen in Figure 27. The polymer is abbreviated as  $\text{BD}_{x/y}$  in the following. Experiments were conducted using three different sets of repeat units (indicated as x and y in Figure 27):  $\text{BD}_{12/9}$ ,  $\text{BD}_{22/13}$  and  $\text{BD}_{16/6}$ . All polymers were purchased from Polymersource (Dorval, Quebec, Canada).

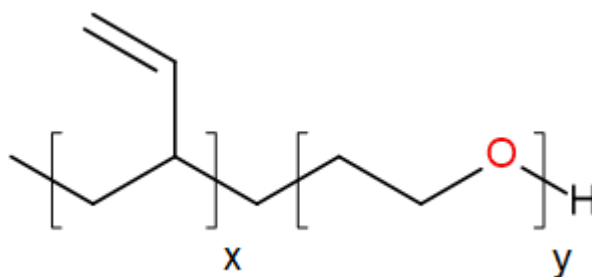


Figure 27 Structure of poly-(buta-1,3-diene)-poly(ethylene oxide).

##### 4.22.1 Polymersome synthesis through solvent exchange

12 mg  $\text{BD}_{16/6}$  were dissolved in 3 mL tetrahydrofuran (THF) to yield a 4 mg / mL polymer solution. Subsequently, 100  $\mu\text{L}$  polymer solution were slowly titrated into 3 mL PBS buffer and stirred over night to evaporate THF. Evaporated water from the PBS solution was refilled to yield the initial volume of 3 mL. As a result, it was possible to calculate the exact polymer concentration. The sample was then manually extruded through a 400 nm PVDF-filter membrane (Avanti Polar Lipids, Alabaster, Alabama, USA) with 30 repetitions to create uniform, unilamellar structures.

##### 4.22.2 Polymersome synthesis through polymer film rehydration

12 mg  $\text{BD}_{16/6}$  were dissolved in 3 mL tetrahydrofuran (THF) to yield a 4 mg / mL polymer solution. Polymersomes were obtained via film rehydration technique. 100  $\mu\text{L}$  polymer solution were pipetted into a 5 mL round bottom flask. The solvent was evaporated under reduced pressure on a rotary evaporator (Büchi, Rotavapor, Switzerland). 2 mL PBS buffer were added into the flask, followed by vigorous shaking (Vortex shaker). The now turbid suspension was then extruded through a 400 nm PVDF-filter membrane (Avanti Polar Lipids, Alabaster, Alabama, USA) with 30 repetitions to create uniform, unilamellar structures.

#### 4.22.3 Polymersome synthesis through Electroformation

Giant unilamellar vesicles (GUVs) were synthesised via electroformation. The polymer BD<sub>12/9</sub>, dissolved in chloroform, was supplemented with one molar percent of 1-palmitoyl-2-{6-[(7-nitro-2-1,3-benzoxadiazol-4-yl)amino]hexanoyl}-*sn*-glycero-3-phosphocholine (NBD PC) as fluorescent dye. NBD PC's structural formula is depicted in Figure 28. 50  $\mu$ L of the chloroform solution were transferred on a glass slide in dropwise fashion. After evaporation of the solvent, the slide was placed under vacuum for 30 minutes. Dried material was rehydrated in either MilliQ water or a 150 mM sucrose solution, depending on experiment. A second glass slide, separated by a 1 mm silicon ring from the former, was placed on top. The slides were placed in Vesicle Prep Pro electroformation device from Nanion Technologies GmbH (Munich, Germany). Electroformation was carried out at a voltage of 3 V and a frequency of 10 Hz for 2 hours at room temperature. The yielding polymersome solution presented a concentration of 1.5 mg/mL and was stored at 4° C until further use.

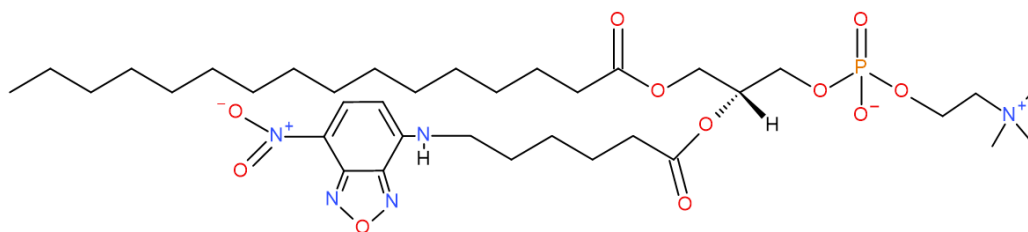


Figure 28 Structural formula of NBD PC.

#### 4.23 Sample preparation for transmission electron microscopy

An *in vitro* synthesis batch of LamB is set up as seen in Table 24. The batch was supplemented with polymersomes synthesized through polymer film rehydration of BD<sub>22/13</sub>. Incubation was carried out at 37° C and 300 rpm for 2 hours. Dialysis against MilliQ water using a membrane with molecular weight cut-off of 100 kDa was performed overnight.

Table 24 IVS batch composition for subsequent TEM analysis.

sample	plasmid [ng]	amino acid mix [ $\mu$ L]	S30 premix [ $\mu$ L]	T7 S30 extract [ $\mu$ L]	MilliQ water [ $\mu$ L]	polymersome solution [ $\mu$ L]
S	2043	5	20	15	0	5
T	2043	5	20	15	0	5

10  $\mu$ L sample were transferred onto a carbon coated 300 mesh copper grid with pioloform support and air dried.

#### 4.24 Transmission electron microscopy

The transmission electron microscopy FEI Tecnai G<sup>2</sup> 200 kV was used to investigate presence and structure of polymersomes after undergoing IVS and dialysis.



#### 4.25 IVS with optimized purification method

Two IVS batches were set up according to Table 25. After 1.5 h of incubation at 37° C and 300 rpm, dialysis with a membrane of 100 kDa molecular weight cut-off was carried out overnight against a 150 mM sucrose solution.

Table 25 IVS composition for optimized purification.

sample	plasmid [ng]	amino acid mix [μL]	S30 premix [μL]	T7 S30 extract [μL]	MilliQ water [μL]	polymersome solution (1.5 μg / μL)
U	2043	5	20	15	5	5 μL (BD <sub>22/13</sub> , 1 % NBD PC)
V	0	5	20	15	8	5 μL (BD <sub>22/13</sub> , 1 % NBD PC)

Aliquots of 10 μL each were denaturized using SDS and further processed via PAGE. The gel was subsequently Coomassie stained.

#### 4.26 Confocal laser microscopy

Two IVS batches were set up, each supplemented with a different polymer. As seen in Table 26, the first two samples (79.3 and 79.4) contained BD<sub>22/13</sub>, the second two (79.5 and 79.6) BD<sub>12/9</sub>.

Table 26 IVS compositions of batches destined for confocal laser microscopy analysis.

sample	plasmid [ng]	amino acid mix [μL]	S30 premix [μL]	T7 S30 extract [μL]	MilliQ water [μL]	polymersome solution (1.5 μg / μL)
W	2050	5	20	15	5	5 μL (BD <sub>22/13</sub> )
X	2050	5	20	15	5	5 μL (BD <sub>22/13</sub> )
Y	2050	5	20	15	5	5 μL (BD <sub>12/9</sub> )
Z	2050	5	20	15	5	5 μL (BD <sub>12/9</sub> )

After incubation at 37° C and 300 rpm for 2 hours, dialysis using a 100 kDa molecular weight cut-off membrane was carried out against MilliQ water and sucrose solution respectively.

Polymersomes were characterized through confocal fluorescence microscopy. The set-up consisted of NIKON's eclipse TE2000-S microscope, combined with Laboratory Imaging's NIS-Elements (version 3.22.11) software. Samples were excited at 460 nm, while emitted photons at 543 nm were recorded.

#### 4.27 SDS-PAGE at reduced voltage

Two IVS batches were set up according to Table 27. After 1.5 h of incubation at 37° C and 300 rpm, the incubation was terminated. Dialysis with a membrane of 100 kDa molecular weight cut off was carried out overnight against a 150 mM sucrose solution.

Table 27 IVS reaction mix composition for subsequent reduced voltage SDS-PAGE.

sample	plasmid [ng]	amino acid mix [μL]	S30 premix [μL]	T7 S30 extract [μL]	MilliQ water [μL]	polymersome solution (1.5 μg / μL)
AA	2043	5	20	15	0	5 μL (BD <sub>16/22</sub> , 1 % NBD PC)
AB	0	5	20	15	8	5 μL (BD <sub>16/22</sub> , 1 % NBD PC)

Aliquots from each sample were treated with SDS and then transferred onto a polyacrylamide gel. PAGE was carried out at a voltage of 100 V. The device was switched off, once the ruler's 30 kDa marker had reached the lower end of the gel. Coomassie staining was followed by an overnight washing step of the gel.

#### 4.28 Fluorescent amino acids

Fluorescently labelled L-lysine-tRNA was provided by Promega's FluoroTect™ Green<sub>Lys</sub> *in vitro* Translation Labeling System (Cat. No. L5001; Lot. No. 0000068957). Per IVS reaction batch 1 μL of labelled lysine solution was (Lys-FT) added as seen in Table 28.

Table 28 IVS mixture composition supplemented with fluorescent lysin.

sample	plasmid [ng]	amino acid mix [μL]	S30 premix [μL]	T7 S30 extract [μL]	MilliQ water [μL]	Lys-FT [μL]
AC	1022	2.5	10	7.5	0	1
AD	0	2.5	10	7.5	4	1

Incubation was carried out for 1.5 hours at 37° C and 300 rpm. Aliquots of 10 μL each were treated with SDS and subsequently transferred onto a polyacrylamide gel. Additionally, a wheat germ IVS batch with a plasmid carrying the CD4 gene was provided from a member of this working group. This sample served as positive control. PAGE was performed to separate proteins according to their size. The gel was then placed under UV-radiation in order to excite the fluorophore.

#### 4.29 Mass spectroscopy

Mass spectroscopic analysis was performed externally by the institute of biochemistry at the University of Natural Resources and Applied Life Sciences, Vienna. Samples underwent tryptic digestion and analysis was carried out on a Bruker maxis 4G Q-TOF mass spectrometer linked to a Dionex Ultimate 3000 LC system.

#### 4.30 Analysis of pBSK(+) sequencing data

The U.S. National Library of Medicine's Basic Local Alignment Search Tool (BLAST)<sup>32</sup> was used for analysing the sequencing data. The option blastx was picked to scan the plasmid's DNA (provided by BIOMATIK) for encoded proteins.

Visualisation and recognition of key features was carried out by SnapGene Viewer (Version 3.2.1) by GSL Biotech LLC.

## 5 Discussion

The initial goal of this thesis was the *in vitro* expression of the membrane protein LamB into a polymeric membrane. As it was eventually discovered, the used plasmid was non-functional as the promotor sequence was displaced and located at a position that did not match the actually ordered sequence. A discussion of potential reasons for failing of previous expression experiments is therefore obsolete. Nonetheless, insights were gained that could prove useful for future experiments in the field of *in vitro* synthesis of membrane proteins into polymersomes. These developed optimisations are discussed in the following, along with reflections about further necessary enhancements of experimental design.

### 5.1 Optimisations

The first improvement was achieved in raising plasmid yields. The initial plasmid mass harvested from one overnight batch of *E. coli* culture was a mere 3.7 µg. As one IVS batch alone requires 1 µg of plasmid, this amount was not suitable for efficient experimentation. Furthermore, the initial DNA concentration of about 75 ng / µL was too low for efficient experimenting, as one IVS batch is limited to a total volume of 50 µL. Therefore, only a limited volume of DNA solution can be added, which requires for a plasmid concentration of several hundred nanogram per microliter.

The amplification protocol was modified by using a pre-culture as inoculum, up-scaling culture volume, enhancing aeration and switching from a DNA preparation kit operating in the µL range to one suited for volumes of mL. The crucial insight, however, was that DNA material remained on the centrifuge tube wall after ultracentrifugation. This pellet, too small to be visible, withstood 'soft' dissolving methods and was inadvertently discarded. Optical DNA measurements were therefore unable to detect DNA. Only after sonication, the pellet could be dissolved. Yields increased by these means reached about 25 µg, a 7-fold improvement at the same expenditure of time. The plasmid concentration was raised to almost 260 ng / µL, which exceeds the initial concentration by more than factor three.

Next to plasmids, suitable polymersomes had to be supplemented to IVS reaction mixtures for experiments described in this work. Unlike plasmids, the issue demanding improvement was not production of efficient amounts, but survivability throughout the *in vitro* synthesis process. As it was discovered, polymersomes filled with MilliQ water did not withstand the IVS environment. The difference in osmotic pressure between the inside of the polymersome and the IVS reaction mix seemed to be the driving force behind the disintegration. To remove the pressure difference across the polymersome membrane, polymersomes were filled with 150 mM sucrose solution. This measure indeed granted polymersomes the ability to sustain integrity throughout incubation, as microscopic analysis showed.

### 5.2 Reflections about possible improvements of future experiment design

Despite abundant plasmid material and sturdy polymersomes, LamB could not be successfully expressed in this work. Experiments involving fluorescently labelled amino acids and protein sequencing suggested, that translation never occurred. It was decided to track down, where exactly the expression of LamB halted by investigating the individual expression steps from DNA template to fully translated protein. First, the sequence of the used plasmid pBSK(+) was analysed, thereby revealing an explanation for the failed expression. The DNA sequence of the vector was corrupted. Not only was the coding sequence truncated, but also not inserted under the control of the desired promotor. Maltoporin was therefore unable to be expressed in

this work. However, while not yielding the initially desired protein, valuable lessons can be drawn from this thesis. The acquired experience allows in retrospect to draft a more efficient experimental design, through which this obstacle could have been detected more quickly.

### 5.2.1 Demand of sceptical handling of material

A refined approach to LamB expression should involve a more critical handling of used material. This includes goods that were manufactured externally, such as pBSK(+). Information given in the manufacturers report should be verified through experimentation to check whether the delivered product matches the order.

Verification of pBSK(+) was for one thing performed through polymerase chain reaction (PCR). PCR was executed using primers designed from sequencing data provided by the manufacturer and not from the actually ordered sequence. This method was therefore unable to detect, whether the desired cDNA was correctly incorporated. Furthermore, these primers were targeting the coding sequence, thus promoter sequences were not probed. This PCR was therefore unable to detect the incorrect orientation of the cDNA inside the plasmid.

Ideally, PCR primers would have been crafted to target the desired T7 promotor as well as the 3' end of the cDNA, as it was defined by the ordered sequence. In this fashion, the successful production of PCR product would suggest not only the correct orientation into the plasmid, but also the correct length.

The second characterization method that was used in this work, digestion by restriction enzymes, suffers from the same flaws as the former. The experiment was designed using data provided by the manufacturer. Namely the choice of restriction enzyme (HindIII), as well as the expected cutting pattern were taken from the plasmid map provided by Biomatik. This experiment therefore investigated the accordance of delivered material and manufacturer's protocol, but not the accordance of ordered specifications and actually delivered material.

Ideally, restriction enzyme digestion would be carried out differently. Analysing the LamB cDNA reveals that several recognition sequences for different restriction endonucleases are present. A well thought out choice of two or more enzymes in addition with the known sequence of the empty pBSK(+) vector would allow to predict the size of resulting DNA fragments. Any deviation from this predicted pattern would suggest an incoherence of the plasmid's sequence.

An even more efficient characterisation method, however, would be DNA sequencing. It would be possible to detect even minor defects as small as one false nucleotide. Ideally, the full vector would be sequenced. The cDNA region, as well as the promotor located upstream of which, would be of highest interest.

### 5.2.2 The importance of efficient detection methods

From the considerations above the importance of critical handling of raw materials becomes evident. This understanding came about only at the end of this thesis, when failed translation was strongly suggested by the use of fluorescent amino acids and the method of protein sequencing. These two protein detection methods are more efficient than protein staining using Coomassie blue, which had been used before. If these techniques were applied earlier, the plasmid's defect would have been detected at an earlier stage of this work. This would have allowed to correct the false sequence and carry on with steps towards successful expression of maltoporin. The selection of potent detection methods is therefore crucial for IVS experiments. To optimise future experiment design, the purposeful selection of detection techniques shall be discussed in the following.

The initially used technique of staining SDS-PAGE gels is prone to yield false positives, due to its low specificity. The poor discrimination and therefore the source of unspecificity is two-fold. First, every protein in the sample is stained. Secondly, detection is carried out by screening for proteins of a specific migration behaviour. Thus, any protein that shares a comparable mass with the target protein can result in a false positive. To reduce the risk of false positives, a detection method should be chosen which responds to a feature of the sought-after protein that is as specific to the target as possible. It should be mentioned at this point that Western blot, a well-established and relatively specific detection method, was not performed in this work, as a suitable antibody targeting LamB was not available.

The use of fluorescent amino acids and protein sequencing through mass spectroscopy fulfils this criterion. In case of the former, only proteins that were synthesized during IVS incubation may have incorporated the labelled amino acids. Therefore only the target protein should be able to give rise to a positive signal. The latter admittedly detects all proteins in the sample, but allows to discriminate them precisely using their amino acid sequence.

Ideally, fluorescently labelled amino acids would have been used as standard detection method for all IVS experiments. A positive signal would strongly suggest that translation of any protein had occurred. The more costly mass spectroscopy, would then be used to clarify whether this signal derived from the protein of interest, or not.

## 6 Supplemental information

### 6.1 Results from protein sequencing via mass spectrometry

Protein	MW [kDa]	pI	MASCOT Score	SC [%]	#Peptides
Elongation factor Tu 2 OS=Escherichia coli O9:H4 (strain HS) GN=tuf2 PE=3 SV=1	43.3	5.2	1985.1	88.6	41
Enolase OS=Escherichia coli (strain K12 / MC4100 / BW2952) GN=eno PE=3 SV=1	45.6	5.2	1149.2	60.2	24
Transcription termination factor Rho OS=Escherichia coli (strain K12) GN=rho PE=1 SV=1	47	6.9	779.9	46.5	19
Maltose-binding periplasmic protein OS=Escherichia coli (strain K12) GN=malE PE=1 SV=1	43.4	5.4	709.2	52	16
Phosphoglycerate kinase OS=Escherichia coli (strain ATCC 8739 / DSM 1576 / Crooks) GN=pgk PE=3 SV=1	41.1	4.9	673.3	42.6	13
Isocitrate dehydrogenase [NADP] OS=Escherichia coli (strain K12) GN=icd PE=1 SV=1	45.7	5	665.6	44.5	17
Cysteine desulfurase OS=Escherichia coli (strain K12 / MC4100 / BW2952) GN=iscS PE=3 SV=1	45.1	5.9	644.1	41.8	17
Adenylosuccinate synthetase OS=Escherichia coli (strain K12 / MC4100 / BW2952) GN=purA PE=3 SV=1	47.3	5.2	585.8	44.7	15
Succinyl-CoA ligase [ADP-forming] subunit beta OS=Escherichia coli (strain K12 / MC4100 / BW2952) GN=sucC PE=3 SV=1	41.4	5.2	572.2	42	15
6-phosphogluconate dehydrogenase, decarboxylating OS=Escherichia coli (strain K12) GN=gnd PE=1 SV=2	51.4	4.9	496.2	38.2	14
S-adenosylmethionine synthase OS=Escherichia coli (strain K12 / MC4100 / BW2952) GN=metK PE=3 SV=1	41.9	5	480.1	40.4	12
Peptidase B OS=Escherichia coli O9:H4 (strain HS) GN=pepB PE=3 SV=1	46.2	5.4	474.6	40.3	12
3-oxoacyl-[acyl-carrier-protein] synthase 2 OS=Escherichia coli (strain K12) GN=fabF PE=1 SV=2	43	5.7	401.8	30.3	10
Citrate synthase OS=Escherichia coli (strain K12) GN=gltA PE=1 SV=1	48	6.2	345.2	27.6	9
Acetate kinase OS=Escherichia coli (strain K12) GN=ackA PE=1 SV=1	43.3	5.8	298.2	35.5	8
Phosphopentomutase OS=Escherichia coli O127:H6 (strain E2348/69 / EPEC) GN=deoB PE=3 SV=1	44.3	5.1	275.5	24.1	9
Fructose-bisphosphate aldolase class 2 OS=Escherichia coli (strain K12) GN=fbaA PE=1 SV=2	39.1	5.5	269.5	17.5	6

Histidyl-tRNA synthetase OS=Escherichia coli (strain K12 / MC4100 / BW2952) GN=hisS PE=3 SV=1	47	5.6	267	17.2	6
Serine hydroxymethyltransferase OS=Escherichia coli O17:K52:H18 (strain UMN026 / ExPEC) GN=glyA PE=3 SV=1	45.3	6	260.6	20.1	8
Tyrosyl-tRNA synthetase OS=Escherichia coli (strain K12 / MC4100 / BW2952) GN=tyrS PE=3 SV=1	47.5	5.5	244.1	19.1	5
GTP-dependent nucleic acid-binding protein engD OS=Escherichia coli (strain K12) GN=engD PE=1 SV=2	39.6	4.7	229.5	20.4	6
3-oxoacyl-[acyl-carrier-protein] synthase 1 OS=Escherichia coli (strain K12) GN=fabB PE=1 SV=1	42.6	5.2	190.8	12.1	5
D-tagatose-1,6-bisphosphate aldolase subunit gatZ OS=Escherichia coli O9:H4 (strain HS) GN=gatZ PE=3 SV=1	47.1	5.4	177.6	14.8	4
Acetylornithine deacetylase OS=Escherichia coli O6:K15:H31 (strain 536 / UPEC) GN=argE PE=3 SV=1	42.2	5.4	153.8	12.3	5
Carbamoyl-phosphate synthase small chain OS=Escherichia coli O6 GN=carA PE=3 SV=2	41.4	6	153	9.7	3
Glutamate-1-semialdehyde 2,1-aminomutase OS=Escherichia coli (strain SMS-3-5 / SECEC) GN=hemL PE=3 SV=1	45.3	4.6	133.8	14.8	5
Chaperone surA OS=Escherichia coli (strain K12) GN=surA PE=1 SV=1	47.3	6.5	132	11.4	4
Argininosuccinate lyase OS=Escherichia coli O127:H6 (strain E2348/69 / EPEC) GN=argH PE=3 SV=1	50.2	5	128.9	14.2	4
Acriflavine resistance protein A OS=Escherichia coli (strain K12) GN=acrA PE=1 SV=1	42.2	8.7	124.2	10.3	3
Aspartate aminotransferase OS=Escherichia coli (strain K12) GN=aspC PE=1 SV=1	43.5	5.5	123.5	22.2	6
NADH-quinone oxidoreductase subunit F OS=Escherichia coli (strain K12) GN=nuoF PE=1 SV=3	493	6.5	122.9	12.8	5
3-phosphoshikimate 1-carboxyvinyltransferase OS=Escherichia coli O17:K52:H18 (strain UMN026 / ExPEC) GN=aroA PE=3 SV=1	46	5.3	109.3	5.6	2
ATP synthase subunit beta OS=Escherichia coli O9:H4 (strain HS) GN=atpD PE=3 SV=1	50.3	4.8	88.4	6.7	3
UDP-N-acetylglucosamine 1-carboxyvinyltransferase OS=Escherichia coli (strain K12 / MC4100 / BW2952) GN=murA PE=3 SV=1	44.8	5.8	78.1	7.9	3
30S ribosomal protein S3 OS=Escherichia coli O139:H28 (strain E24377A / ETEC) GN=rpsC PE=3 SV=1	26	11	71.7	12.9	2
Cell division protein FtsZ OS=Escherichia coli (strain K12) GN=ftsZ PE=1 SV=1	40.3	4.5	68	7.3	2
ATP-dependent Clp protease ATP-binding subunit ClpX OS=Escherichia coli (strain K12 / MC4100 / BW2952) GN=clpX PE=3 SV=1	46.3	5.1	59.8	4.7	2



D-3-phosphoglycerate dehydrogenase OS=Escherichia coli (strain K12) GN=serA PE=1 SV=2	44.1	5.9	53.5	7.1	2
Biotin carboxylase OS=Escherichia coli (strain K12) GN=accC PE=1 SV=2	49.3	6.7	52.6	6	2
UDP-glucose 6-dehydrogenase OS=Escherichia coli O6 GN=ugd PE=3 SV=1	43.6	6	50.2	5.9	2
Asparaginyl-tRNA synthetase OS=Escherichia coli O9:H4 (strain HS) GN=asnS PE=3 SV=1	52.5	5	48.7	3.6	2
Molybdopterin molybdenumtransferase OS=Escherichia coli (strain K12) GN=moeA PE=1 SV=1	44	4.9	36.3	9.5	2

## 7 Bibliography

- 1 Sachse, R., Quast, R. B., Son nabend, A., Stech, M. & Kubick, S. Membranproteinsynthese: Zellfrei geht's schneller! *BIOspektrum*, 570-573 (2014).
- 2 Lodish, H. *et al.* *MOLECULAR CELL BIOLOGY*. 6 edn, 17 (Freeman, 2008).
- 3 Waters, C. M. & Bassler, B. L. QUORUM SENSING: Cell-to-Cell Communication in Bacteria. *Cell and Developmental Biology* **21**, 319-346 (2005).
- 4 Nelson, G. *et al.* Mammalian Sweet Taste Receptors. *Cell Press* **106**, 381-390 (2001).
- 5 Graff, A., Sauer, M., Van Gelder, P. & Meier, W. Virus-assisted loading of polymer nanocontainer. *PNAS* **99**, 5064 - 5068 (2002).
- 6 Sauer, K., Camper, A. K., Ehrlich, G. D., Costerton, J. W. & Davies, D. G. *Pseudomonas aeruginosa* Displays Multiple Phenotypes during Development as a Biofilm. *Journal of Bacteriology* **184**, 1140-1154 (2002).
- 7 Ranquin, A. & Van Gelder, P. Maltoporin: sugar for physics and biology. *Research in Microbiology* **155**, 611-616 (2004).
- 8 Berkane, E. *et al.* Nanopores: maltoporin channel as a sensor for maltodextrin and lambda-phage. *Journal of Nanobiotechnology* **3** (2005).
- 9 Laszlo, A. H. *et al.* Decoding long nanopore sequencing reads of natural DNA. *Nature Biotechnology* **32**, 829-834 (2014).
- 10 Rigaud, J.-L. & Lévy, D. in *METHODS IN ENZYMOLOGY* Vol. 372 Ch. 4, (Elsevier Inc. , 2003).
- 11 Lin, S.-H. & Guidotti, G. Purification of Membrane Proteins. *Methods in Ezymology* **463**, 619-629 (2009).
- 12 Sachse, R. *et al.* Synthesis of membrane proteins in eukaryotic cell-free systems. *Life Sci.* **13**, 39-48 (2013).
- 13 Bermudez, H., Bannan, A. K., Hammer, D. A., Bates, F. S. & Discher, D. E. Molecular Weight Dependence of Polymersome Membrane Structure, Elasticity, and Stability. *Macromolecules* **35**, 8203-8208 (2002).
- 14 Lee, J. S. & Feijen, J. Polymersomes for drug delivery: Design, formation and characterization. *Journal of Controlled Release* **161**, 473-483 (2012).
- 15 Zemella, A., Thoring, L., Hoffmeister, C. & Kubick, S. Cell-Free Protein Synthesis: Pros and Cons of Prokaryotic and Eukaryotic Systems. *ChemBioChem* **16**, 2420-2431 (2015).
- 16 e.V., F.-G. z. F. d. a. F. (2013).
- 17 Junge, F. *et al.* Advances in cell-free protein synthesis for the functional and structural analysis of membrane proteins. *New Biotechnology* **28**, 262-271 (2011).
- 18 e.V., F.-G. z. F. d. a. F. (2013).
- 19 Tan, S., Tan, H. T. & Chung, M. C. M. Membrane proteins and membrane proteomics. *Proteomics* **8**, 3924-3932 (2008).
- 20 Graff, A. *Insertion of Membrane Proteins in Artificial Polymer Membranes* PhD thesis, Universität Basel, (2004).
- 21 **Information, N. C. f. B.** maltoporin [*Shigella sonnei*] NCBI Reference Sequence: WP\_052994967.1, <[https://www.ncbi.nlm.nih.gov/protein/WP\\_052994967.1](https://www.ncbi.nlm.nih.gov/protein/WP_052994967.1)> (2015).
- 22 Swaminathan , J. Vol. 800 x 600 (65 kb) (ed PDB\_1mal\_EBI.jpg) (commons.wikimedia.org, 2009).
- 23 QIAGEN® Plasmid Mini, Midi, and Maxi Kits - Quick-Start Protocol, <<https://www.qiagen.com/us/resources/download.aspx?id=c164c4ce-3d6a-4d18-91c4-f5763b6d4283?en>> (2011).
- 24 Damiani, S. *et al.* Inspired and stabilized by nature: ribosomal synthesis of the human voltage gated ion channel (VDAC) into 2D-protein-tethered lipid interfaces. *Biomaterials Science* **3**, 1406-1413 (2015).
- 25 Rath, A., Glibowicka, M., Nadeau, V. G., Chen, G. & Deber, C. M. Detergent binding explains anomalous SDS-PAGE migration of membrane proteins. *PNAS* **106**, 1760 - 1765 (2007).

- 26 Brinas, L., Zarazaga, M., Sáenz, Y., Ruiz-Larrea, F. & Torres, C.  $\beta$ -Lactamases in Ampicillin-Resistant *Escherichia coli* Isolates from Foods, Humans, and Healthy Animals *Antimicrobial Agents and Chemotherapy* **46**, 3156-3163 (2002).
- 27 Sequence Manipulation Suite: Reverse Translate,  
<[http://www.bioinformatics.org/sms2/rev\\_trans.html](http://www.bioinformatics.org/sms2/rev_trans.html)> (
- 28 Scientific, T. F. <https://www.thermofisher.com/us/en/home/brands/thermo-scientific/molecular-biology/molecular-biology-learning-center/molecular-biology-resource-library/thermo-scientific-web-tools/tm-calculator.html>, 2016).
- 29 Bertani, G. (1951).
- 30 invitrogen. in *General information and protocols for using the NuPAGE® electrophoresis system* (2010).
- 31 Zapf, T. *et al.* Nanoscopic leg irons: harvesting of polymer-stabilized membrane proteins with antibody-functionalized silica. *Biomater. Sci* **3**, 1247–1314 (2015).
- 32 <http://blast.ncbi.nlm.nih.gov/Blast.cgi>.